TECHNISCHE UNIVERSITÄT MÜNCHEN

Fakultät für Medizin

Inhibition of Epigenetic Readers to block adaptive rewiring induced by targeted therapies in pancreatic cancer

KATJA ANDREA ASCHERL

Vollständiger Abdruck der von der

Fakultät für Medizin der Technischen Universität München

zur Erlangung des akademischen Grades einer

Doktorin der Medizin (Dr. med.)

genehmigten Dissertation.

Vorsitz: apl. Prof. Dr. Bernhard Haslinger

Prüfende der Dissertation: 1. Prof. Dr. Günter Schneider

2. Prof. Dr. Maximilian Reichert

3. apl. Prof. Dr. Alexander Novotny

Die Dissertation wurde am 11.10.2021 bei der Technischen Universität München eingereicht und durch die Fakultät für Medizin am 12.07.2022 angenommen.

Acknowledgement

Foremost I would like to express my sincere gratitude to Prof. Dr. med. Günter Schneider for giving me the opportunity to work on such an interesting research topic. Most of all I am thankful for his productive inputs combined with his broad knowledge, which he was always willing to share.

I want to thank Prof. Dr. med. Maximilian Reichert, who assumed the role as my mentor.

Furthermore, I am particularly grateful for my incredible supervisor M.Sc. Christian Schneeweis for his never-ending patience answering all my questions, for providing helpful research expertise, for his motivation and his valuable feedback during all the periods of this thesis. I could not imagine having a more excellent advisor for my research work as him.

Dr. rer. nat. Zonera Hassan deserves a special word of gratitude for her advancing assistance in the lab and her helpful advice whenever I was faced with an issue.

As well thanks to all members of AG Schneider including for their warm welcome, the friendly help with every problem and the great time during and after work.

Finally, for excellent proof-reading and useful comments, I want to thank Prof. Dr. med. Günter Schneider, Christian Schneeweis and Dr. Claudia Wutz.

Thank you!

Table of contents

Abstract

Pancreatic ductal adenocarcinoma (PDAC) still carries a dismal prognosis with an overall five-year survival of 10 % and is the fourth leading cause of the cancer-associated deaths in the Western World (Siegel et al., 2021). Due to the late onset of nonspecific symptoms, the tumor diagnosis is often made in an advanced stage of the disease. Moreover, the current therapies, against which the tumor is largely resistant, need urgent improvement. A nearly universal KRAS (Kirsten rat sarcoma 2 viral oncogene homolog) mutation is one of the main drivers in PDAC oncogenesis, resulting in a constitutive activation of downstream signaling pathways. Although pre-clinical data show that the PI3K (phosphoinositid-3-kinase)-AKT-MTOR pathway, downstream of KRAS, is a relevant pathway for therapeutic intervention, clinical trials have failed so far. Therefore, a more detailed molecular understanding on how PDAC escapes PI3K-AKT-MTOR inhibition is needed.

Previous work in our group demonstrated that the MTOR knockout in established PDAC cell lines had a significant effect on cell growth, but exclusively in a cytostatic manner. Additionally, the cells establish an adaptive rewiring of oncogenic signaling leading to an increased activation of the RAS-MEK-ERK- and the AKT-pathway. The problem of arising secondary resistance mechanism is one of the main issues of failed targeted therapies in the clinic so far.

After targeting RTK (receptor tyrosine kinase) activation or the upregulation of NF-κB upon MTOR blockage, synergistic effects could not be shown. A comprehensive database based on the concept of synthetic lethality (SL) harboring a large set of SL pairs predicted MTOR and MYC as a promising SL pair. This led to utilizing epigenetic inhibitors like BET inhibitors (BETi), which indirectly target MYC to block the adaptive rewiring. In murine PDAC cells it was shown that MTOR-deficiency is linked to an increased BETi sensitivity. Furthermore, the investigated BETi acted synergistically with the MTOR inhibitor (MTORi) INK-128, even though the exact mechanism of the synergistic effect remains unclear.

Further research will be required to clarify the mechanism of the adaptive rewiring upon the MTOR inhibition and to improve the understanding of the molecular processes behind the synergisym between MTOR and MYC in PDAC.

Zusammenfassung

Das duktale Adenokarzinom des Pankreas (PDAC) ist noch immer eine schwerwiegende Diagnose mit einer 5-Jahres-Gesamtüberlebensrate von 10 % und die vierthäufigste Ursache für tumorbedingte Todesfälle in der westlichen Welt (Siegel et al., 2021). Aufgrund der spät eintretenden sowie unspezifischen Symptome wird die Diagnose häufig erst im fortgeschrittenen Stadium gestellt. Die derzeit angewandten Therapien müssen dringend verbessert werden, da PDAC gegen diese weitgehend resistent ist. Der Haupttreiber der PDAC-Onkogenese ist eine nahezu universale KRAS (Kirsten rat sarcoma 2 viral oncogene homolog) -Mutation, die zu einer konstitutiven Aktivierung der nachgeschalteten Signalwege führt. Obwohl präklinische Daten zeigen, dass der PI3K-AKT-MTOR-Signalweg, nachgeschaltet von KRAS, ein relevanter Angriffspunkt für therapeutische Interventionen ist, sind klinische Studien bisher gescheitert. Daher ist ein detaillierteres molekulares Verständnis erforderlich, wie es der Tumor meistert die Hemmung des PI3K-AKT-MTOR-Signalweges zu umgehen.

Frühere Arbeiten unserer Gruppe konnten zeigen, dass ein MTOR-Knockout in etablierten Pankreaskarzinomzelllinien einen signifikanten Einfluss auf das Zellwachstum hat, jedoch ausschließlich in zytostatischer Weise. Zusätzlich adaptieren die Zellen mit einer Neuverschaltung der onkogenen Signalübertragung, welche zu einer erhöhten Aktivierung des RAS-MEK-ERK- und des AKT-Signalweges führt. Das Auftreten sekundärer Resistenzmechanismen ist eine Hauptursache fehlgeschlagener zielgerichteter Therapien in der Klinik.

Die gezielte Blockade der aktivierten RTK oder des NF-κB – Signalweges in Kombination mit Hemmung von MTOR zeigte keine synergistischen Effekte. Demnach führte die Suche in einer Datenbank für synthetische Letalität (SL) zu MYC als vielversprechendstem SL-Paar mit MTOR. Dies führte zur Verwendung epigenetischer Inhibitoren wie beispielsweise BET-Inhibitoren (BETi), mit MYC als indirekten Angriffspunkt, um die adaptive Neuverschaltung der onkogenen Signalwege zu blockieren. In murinen PDAC-Zellen konnte ein Zusammenhang zwischen MTOR-Defizienz und erhöhter BETi-Empfindlichkeit nachgewiesen

werden. Darüber hinaus wirkte die untersuchte BET-Blockade synergistisch mit dem MTOR Inhibitor (MTORi) INK-128, obwohl der genaue Mechanismus des synergistischen Effekts unklar bleibt.

Um den Mechanismus der adaptiven Neuverschaltung nach Blockade von MTOR und die molekularen Prozesse des Synergismus zwischen MTOR und MYC in PDAC zu verstehen ist weitere Forschungsarbeit erforderlich.

List of abbreviations

α	*alpha*
%	*percent*
°C	*degree celcius*
4EBP1	*inhibitory 4E-binding protein 1*
ADP	*adenosine diphosphate*
AKT	*Ak strain transforming*
APS	*ammonium persulfate*
ATP	*adenosine triphosphate*
BET	*bromodomain and extraterminal domain*
BETi	*BET inhibitor*
bp	*base pairs*
BRCA	*breast cancer gene*
BRD	*bromodomain*
BRD2	*bromodomain-containing protein 2*
BRD3	*bromodomain-containing protein 3*
BRD4	*bromodomain-containing protein 4*
BRDT	*bromodomain testis associated*
BrdU	*5-bromo-2'-deoxyuridine*
BSA	*bovine serum albumin*
cDNA	*complementary DNA*
CI	*combination index*
CK2	*casein kinase 2*
cm	*centimeter*
CO2	*carbon dioxide*
Cre	*cAMP responsive element*
CS	*confidence score*

CT	*cycle thershold*
Ctrl	*control*
DEPTOR	*DEP domain containing MTOR-interacting protein*
DMEM	*Dulbecco's Modified Eagle's Medium*
DMSO	*dimethyl sulfoxide*
DNA	*deoxyribonucleic acid*
dNTP	*desoxynucleotide*
EDTA	*ethylenediaminetetraacetic acid*
EIF4EBP1	*eIF4E-binding protein 1*
ERK	*extracellular-signal regulated kinase*
ERK1/2	*extracellular signal-regulated kinases 1 and 2*
EtBr	*ethidium bromide*
EtOH	*ethanol*
FACS	*fluorescence-activated cell sorting*
FBXO32	*F-box only protein 32*
FCS	*fetal bovine serum, fetal calf serum*
fwd	*forward*
g	*gram*
GAP	*GTPase-activating protein*
GDP	*guanosine diphosphate*
GEF	*guanine nucleotide exchange factor*
GSEA	*gene set enrichment analysis*
GTP	*guanosine triphosphate*
h	*hour(s)*
IC50	*half maximal inhibitory concentration*
IGF1	*insulin-like growth factor 1*
IGF1R	*insulin-like growth factor 1 receptor*
IKBKE	*inhibitor of nuclear factor kappa-B inhibitor of nuclear factor kappa-B kinase subunit epsilon*
INK-128	*sapanisertib*

IPMN	*intraductal papillary mucinous neoplasm*
IR	*insulin receptor*
IκB	*inhibitor of κB protein*
k, kilo	*thousand*
KCM	*KCl $CaCl_2$ $MgCl_2$*
kDa	*kilodalton*
KRAS	*kirsten rat sarcoma 2 viral oncogene homolog*
m	*thousandth*
M	*molar*
mA	*milliampere*
MAPK	*mitogen-activated protein kinase*
MCN	*mucinous cystic pancreatic neoplasm*
MEK	*mitogen-activated protein kinase kinase*
mg	*milligram*
min	*minute*
ml	*milliliter*
mLST8	*mammalian lethal with Sec13 protein 8*
mM	*millimolar*
mRNA	*messenger RNA*
mSin1	*mammalian stress-activated map kinase-interacting protein 1*
MTOR	*mechanistic target of rapamycin*
mTORC1	*MTOR complex 1*
mTORC2	*MTOR complex 2*
MTORi	*MTOR inhibitor*
MTT	*3-(4,5-dimethylthiazol-2-yl-)-2,5-diphenyltetrazolium bromide*
MYC	*myelocytomatosis oncogene cellular homolog*
NEMO	*NF-κB essential modulator*
NES	*normalized enrichment score*
NF1	*neurofibromatosis type I*
NF-κB	*NF-kappaB*
NIK	*NF-κB inducing kinase*
nm	*nanometer*
nM	*nanomolar*

ns	*not significant*
OXPHOS	*oxidative phosphorylation*
p	*phospho*
p120GAP	*p120 GTPase-activating protein*
p38 MAPK	*p38 mitogen-activated protein kinase*
p53	*protein 53*
PanIN	*pancreatic intraepithelial neoplasia*
PBS	*phosphate buffered saline*
PCR	*polymerase chain reaction*
PDAC	*pancreatic ductal adenocarcinoma*
PDK1	*phosphoinositide-dependent kinase 1*
Pen Strep	*penicillin/streptomycin*
PH	*pleckstrin homology*
PI	*propidium iodide*
PI3K	*phosphoinositid-3-kinase*
PIP_2	*phosphatidylinositol (4,5)-bisphosphate*
PIP_3	*phosphatidylinositol (3,4,5)-trisphosphate*
PLC-ε	*phospholipase C epsilon*
PRAS40	*proline rich AKT substrate 40 kDa*
PROTAC	*proteolysis targeting chimeras*
protor1/2	*protein observed with rictor 1 and 2*
PTEN	*phosphatase and tensin homolog*
qPCR	*quantitative real-time PCR*
Rac	*ras-related C3 botulinum toxin substrate*
RAF	*rapidly accelerated fibrosarcoma*
RalGDS	*ral guanine nucleotide dissociation stimulator*
rapalogs	*rapamycin analogs*
raptor	*regulatory assosciated protein of MTOR*
Rassf1	*ras association domain-containing protein 1*
rel.	*relative*
rev	*reverse*
RHD	*Rel homology domain*

Rheb	*ras-homolog enriched in brain*
Rho	*ras homology*
Rictor	*rapamycin-insensitive companion of MTOR*
RIPA	*radioimmunoprecipitation assay*
RNA	*ribonucleic acid*
RNA-Seq	*RNA-sequencing*
RSK	*ribosomal S6 kinase*
RT	*reverse transcription*
RTK	*receptor tyrosine kinase*
S6K	*ribosomal protein S6 kinase*
SD	*standard deviation*
SDS	*sodium dodecyl sulfate*
sec	*second*
Ser, S	*serine*
SL	*synthetic lethality*
SNP	*single-nucleotide polymorphism*
ß	*beta*
TAE	*TRIS-Acetat-EDTA*
TBK1	*TANK-binding kinase 1*
TEMED	*N,N,N',N'-Tetramethylenthylenediamine*
TF	*transcription factor*
Thr, T	*threonine*
TNFα	*tumor necrosis factor alpha*
TNFAIP3 / A20	*tumor necrosis factor a-induced protein 3*
TRIS	*tris-(hydroxymethyl)-aminomethane*
TSC1/2	*tuberous sclerosis complex 1/2*
Tyr	*tyrosine*
UMIs	*unique molecular identifiers*
USP11	*ubiquitin carboxyl-terminal hydrolase 11*
UV	*ultra violet*

V	*volt*
v/v	*volume per volume*
VEGFR3	*vascular endothelial growth factor receptor 3*
VHL	*Von Hippel-Lindau tumor suppressor*
vs.	*versus*
w/v	*weight per volume*
x	*times*
YAP1	*yes-associated protein 1*
µ, micro	*millionth*
µg	*microgram*
µl	*microliter*
µM	*micromolar*

1 Introduction

1.1 Pancreatic cancer

Pancreatic ductal adenocarcinoma (PDAC) is one of the deadliest malignancies with a poor prognosis reflected by a 5-year-survival of only 10 % (Siegel et al., 2021). Due to the lack of effective treatment options, including a lack of targeted therapies with clear impact for patient survival in the clinic, PDAC has one of the highest mortality rates of all cancers. Currently it is the third most common cancer-related death in the US (Rahib et al., 2021) with estimated 60,430 new diagnoses and 48,220 deaths in 2021. As a result of the ageing population and lack of therapeutic options the incidence and deaths are expected to increase dramatically, so that by the year 2030, PDAC is projected to become the second leading cause of cancer-related death in the Western world (Quante et al., 2016; Rahib et al., 2014; Rahib et al., 2021).

Difficulties in PDAC prevention and early diagnosis at a curable stage as well as late nonspecific clinical presentation furthermore contributes to the dismal prognosis. Initial detection of the malignant tumor usually takes place in advanced stages. Today the only curative therapy option is surgical resection, which is not possible in the majority (85 %) of patients (Kleeff et al., 2016).

Although there are numerous studies on etiology, the cause is often unknown (Kleeff et al., 2016). The two major risk factors are chronic pancreatitis and age. Most of the diagnoses are made in >50 years old patients, with peak incidence in the seventh and eighth decades of life. Besides that, a preventable risk factor is tobacco smoking that doubles the chance to develop PDAC (Bosetti et al., 2012; Parkin, 2011; Whiteman et al., 2015). There are several other factors that might affect the disease like obesity, low physical activity, heavy alcohol consumption and diabetes mellitus but not all of them are proven (Kleeff et al., 2016).

Among all pancreatic malignancies, PDAC is the most common pancreatic tumor representing approximately 85 % of the cases. The rarer types of pancreatic neoplasms include acinar carcinomas and neuroendocrine tumors. According to the classical progression model PDAC evolves in a stepwise fashion through a series of precursor lesions, the so called pancreatic intraepithelial neoplasias (PanINs) that are characterized by well-defined morphology and genetic

alterations (Melo et al., 2016). In addition, PDAC can arise from alternative lesion including intraductal papillary mucinous neoplasm (IPMN) or mucinous cystic pancreatic neoplasm (MCN) (Melo et al., 2016).

1.2 Oncogenic signaling in PDAC

More than 90 % of PDAC patients harbor mutations in the KRAS (kirsten rat sarcoma 2 viral oncogene homolog) oncogene, a small GTPase of the RAS family (Knudsen et al., 2016). KRAS is a monomeric G-protein that binds GDP in its inactive form. For activation, GEFs (guanine nucleotide exchange factor) are required to exchange GDP for GTP. GAPs (GTPase-activating protein) increase the conversion rate of GTP to GDP by stimulating the GTPase activity and thereby switching KRAS off. One single substitution of amino acid at G12, G13 or Q61 is sufficient for leading to mutated KRAS, that is insensitive for GAP (Agarwal & Saif, 2014). Consequently, mutant KRAS is continuously activated in a GTP-bound state. This is uniquely sufficient to initiate PanIN formation, which can spontaneously progress to an aggressive metastatic PDAC (Guerra et al., 2007; Hingorani et al., 2003). Due to the continuous activation of oncogenic KRAS, various signaling pathways like canonical RAF/MEK/ERK (rapidly accelerated fibrosarcoma/mitogen-activated protein kinase/extracellular-signal regulated kinases), PI3K/AKT (phosphoinositide 3-kinase/Ak strain transforming), RalGDS/p38 MAPK (ral guanine nucleotide dissociation stimulator/p38 mitogen-activated protein kinase), Rac and Rho (ras-related C3 botulinum toxin substrate and ras homology), Rassf1 (ras association domain-containing protein 1), NF1 (neurofibromatosis type I), p120GAP (p120 GTPase-activating protein) and PLC-ε (phospholipase C epsilon) are induced (Eser et al., 2013). In PDAC, two main driver pathways downstream of the KRAS oncogene are the canonical MEK-ERK and the PI3K/AKT pathway. Through active PI3K, phosphatidylinositol (4,5)-bisphosphate (PIP_2) is transformed into the second messenger phosphatidylinositol (3,4,5)-trisphosphate (PIP_3). Consequently, at the membrane PIP_3 binds a pleckstrin homology domain, including AKT or PDK1. The kinase activity of AKT/PKB is fully stimulated via PDK1 that phosphorylates AKT Thr308 and mTORC2 phosphorylating at Ser473 (Stratikopoulos & Parsons,

2016). This leads to the phosphorylation of several proteins, which support cell growth and survival (Castellano & Downward, 2011). Another well studied downstream pathway of RAS is the RAF-MEK-ERK signaling pathway. The phosphorylated RAF (serine/threonine kinase) activates MEK that, in turn phosphorylates extracellular signal-regulated kinases 1 and 2 (ERK1/2) (Castellano & Downward, 2011). Activation of these pathways leads to tumor development and progression by regulating growth, proliferation, metabolism and survival.

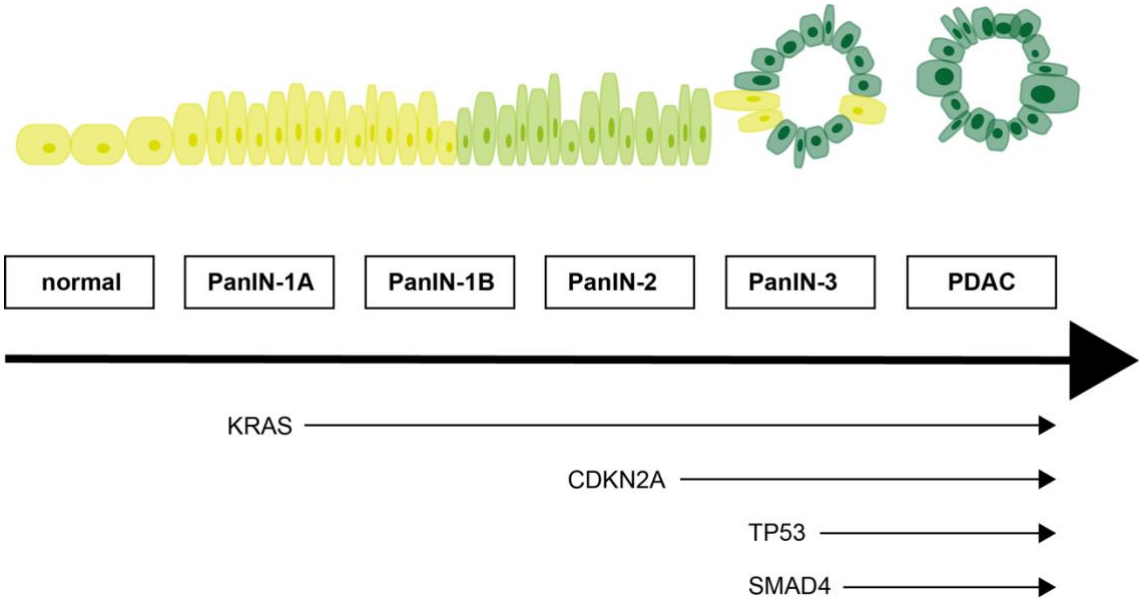

Figure 1. Oncogenes and tumor suppressor genes in PDAC development (Vincent et al., 2011).

1.3 MTOR

The mechanistic target of rapamycin (MTOR) is an important serine/threonine protein kinase and downstream target of the PI3K signaling pathway (Saxton & Sabatini, 2017) that is implicated in the progression of cancer, type II diabetes mellitus, obesity, neurodegeneration and aging. It is included in two protein complexes, the MTOR complex 1 (mTORC1) and 2 (mTORC2). The kinase coordinates cell growth and metabolism. Both MTOR complexes contain 6 or 7 components. The shared elements are the catalytic MTOR subunit, mLST8 (mammalian lethal with SEC thirteen 8), DEPTOR (DEP domain containing

MTOR-interacting protein) (Peterson et al., 2009) and the Tti1/Tel2 complex (Kaizuka et al., 2010). Furthermore, mTORC1, whose activity is controlled by growth factors, also includes specific elements raptor (regulatory assosciated protein of MTOR) and PRAS40 (proline rich AKT substrate 40 kDa). It coordinates the balance between anabolism and catabolism and promotes protein, lipid and nucleotide synthesis by phosphorylating its downstream targets, including ribosomal S6 kinase (RSK) and eIF4E-binding protein 1 (EIF4EBP1). In contrast to mTORC1, Rictor (rapamycin-insensitive companion of MTOR), mSin1 (mammalian stress-activated map kinase-interacting protein 1) (Frias et al., 2006) and protor1/2 (protein observed with rictor 1 and 2) (Pearce et al., 2011) are exclusively part of mTORC2 (Saxton & Sabatini, 2017). mTORC2 is stimulated by insulin/PI3K signaling and controls cytoskeletal organization, proliferation and survival of eukaryotic cells through phosphorylating several members of the AGC (PKA/PKG/PKC) family of protein kinases.

There are several upstream regulators of mTORC1. The major input comes from growth factors (such as insulin and IGF1), stress, energy status (e.g. ATP/ADP ratio) and amino acids (leucine and arginine). The key upstream regulator of mTORC1 is TSC1/2 (tuberous sclerosis complex 1/2) that functions as a GTPase-activation protein for the RHEB GTPase (ras-homolog enriched in brain). Through direct interaction, RHEB in the GTP-bound form stimulates the kinase activity of mTORC1 (Inoki et al., 2003).

As response to various stimuli, PI3K catalyzes the formation of PIP_3. This membrane lipid second messenger recruits downstream effectors such as the AKT family members. AKT consists of the N-terminal pleckstrin homology (PH) domain and two key residues Thr308 and Ser473 (Sarbassov et al., 2005). PDK1 phosphorylates Thr308 and mTORC2 the Ser473 residue to activate AKT. Besides phosphorylating multiple substrates like TSC2, AKT can also activate mTORC1, which results in phosphorylation of ribosomal protein S6 kinase (S6K) and inhibitory 4E-binding protein 1 (4EBP1) to activate protein translation. However, the activated mTORC1 also forms an important feedback loop that results in the inhibition of the PI3K-AKT pathway (Song et al., 2012).

In several human cancers, various upstream parts of mTORC1 and mTORC2 are mutated that lead to activation of MTOR. In 60 % of PDAC patients, the PI3K/AKT signaling is deregulated (Murthy et al., 2018). Moreover, 20 % of PDAC show

hyperactivation of MTOR characterized by the phosphorylation of Ser2448, which is connected with poor survival (Morran et al., 2014). Therefore, it can be concluded that MTOR is a relevant node in the integration of different signaling pathways and a potential therapeutic target (Kong et al., 2016; Morran et al., 2014). Although initial *in vitro* and *in vivo* studies have generally failed due to secondary resistances upon MTOR inhibition (Iriana et al., 2016), combined MTOR pathway inhibition may offer a viable alternative (Hassan et al., 2018).

1.4 MTOR inhibitors

Meanwhile, more than 40 MTOR inhibitors (Table 1), which are distinguished in various groups have reached different clinical trials (Janku et al., 2018). Allosteric MTOR inhibitors like Rapamycin and rapalogs (rapamycin analogs) bind to FKBP12 (FK506 binding protein) and the FRB (FKBP-rapamycin-binding) domain of MTOR, thus inhibiting the kinase activity of mTORC1. The Food and Drug Administration has approved temsirolimus and everolimus for treatment of, for example, advanced renal cell carcinoma and pancreatic neuroendocrine tumors. Some patients with other tumor types such as mesothelioma or endometrial cancer have shown responses, but less successful than expected (Hassan et al., 2014). In PDAC, rapalogs failed to demonstrate a benefit in the clinic (Garrido-Laguna et al., 2010; Morran et al., 2014), most likely due to the presence of multiple negative feedback loops that limit the efficacy of rapalogs (Laplante & Sabatini, 2012). One major negative feedback loop is due to the fact that only mTORC1 is inhibited, so mTORC2 can phosphorylate and activate AKT. Nevertheless, one *in vivo* study in intestinal tumors has demonstrated that rapamycin treatment can lead to a significantly longer survival, tumor shrinkage and a loss of proliferation within the tumor. In sum, this data points to the existence of an MTORi sensitive subtype (Faller et al., 2015). To avoid feedback activation, dual MTOR kinase inhibitors (ATP-competitive inhibitors) that compete with ATP in the catalytic site of MTOR and thereby directly inhibit the catalytic activity of both MTOR complexes were developed and are now tested in the clinic. Besides blocking both arms of the MTOR signaling these dual MTORi also prevent the translational initiation due to targeting 4E-BP1. Genetic inactivation

of mTORC2 *in vivo* impaired the development and progression of PanIN and prolonged the survival of the genetically engineered mice. In addition, pharmacological inhibition of mTORC1/2 with the dual MTORi AZD2014 impaired pancreatic tumor formation and prolonged survival in mice (Driscoll et al., 2016). Due to the fact that resistances occurred again after the dual MTOR inhibition, these mechanisms have to be understood more precisely and there is certainly a need for dual inhibition along the MTOR pathway.

Table 1. MTOR inhibitors. *(Janku et al., 2018)*

Drug class	Drug	Stage of clinical development
mTORC1 inhibitors	Temsirolimus	Approved for treatment of advanced-stage renal cancer
	Everolimus	Approved for treatment of advanced-stage renal cancer, advanced-stage hormone receptor positive breast cancer (postmenopausal women), well-differentiated neuroendocrine tumors, renal angiomyolipoma, subependymal giant cell astrocytoma
	Ridaforolimus	Phase III trial for advanced-stage soft-tissue sarcoma
	Nabrapamycin	Phase II study for MTOR-mutated advanced-stage cancers, perivascular epitheloid cell tumors, other sarcomas
mTORC1 and mTORC2 inhibitors	Vistusertib	Phase II study for RICTOR-amplified tumors and a variety of advanced-stage cancers
	AZD8055	Phase I study for advanced-stage solid tumors and lymphoma
	Sapanisertib (INK-128)	Phase II study for advanced-stage solid cancers
	CC-223	Phase II study for lymphoma
	OSI-027	Phase II study for head and neck squamous cell carcinoma

1.5 Epigenetic readers

Epigenetics are heritable changes in gene function that are independent of DNA sequence variation. In general, epigenetic regulation is a reversible, dynamic process whose regulators can be distinguished in epigenetic writers, readers and erasers. While epigenetic writers catalyze the addition, erasers remove epigenetic marks. Epigenetic readers recognize specific marks and bind to chromatin or histone modifications (Bennett & Licht, 2018). Altogether, they alter the chromatin, the complex of DNA and histones, which can be present in different states. The heterochromatin is highly condensed and contains the inactive genes, whereas the euchromatin has an open chromatin architecture with the active genes. Epigenetic readers are involved in several nuclear processes such as DNA repair, transcription and replication. Bromodomains were first identified in the early 1990s in the brahma gene of Drosophila melanogaster (Tamkun et al., 1992). In humans, 8 structural subfamilies were found with a total of 61 bromodomains in 46 different proteins (Pérez-Salvia & Esteller, 2017). The bromodomain and extraterminal domain (BET) proteins (about 110 amino acids) regulate gene transcription, function as cell cycle regulators and are epigenetic readers. This family in humans consists of BRD2 (Bromodomain-containing protein 2), BRD3 (Bromodomain-containing protein 3), BRD4 (Bromodomain-containing protein 4), which are ubiquitously expressed and BRDT (bromodomain testis associated), which is only expressed in germ cells, but all of them contain two N-terminal BRDs (Stratikopoulos & Parsons, 2016). BET proteins in general recognize and bind acetylated-lysine residues in histones and facilitate the recruitment of different transcription factors to chromatin allowing effective transcriptional elongation of genes by RNA polymerase II (Stathis & Bertoni, 2018).

1.6 BET inhibitors

BET inhibitors bind competitively to BRDs and consequently prevent the protein-protein-interaction between BET proteins, acetylated histones and transcription factors. They were initially developed by Yoshitomi Pharmaceuticals in the early

1990s (Filippakopoulos et al., 2010) and the first reported drug of these anti-tumor agents was JQ1 (thieno-triazolo-1,4-diazepine), which displaces BET proteins from chromatin through competitive binding of BET bromodomains (Pérez-Salvia & Esteller, 2017).

There are many published studies demonstrating the efficacy of JQ1 in various malignancies like lung cancer (Lockwood et al., 2012; Shimamura et al., 2013), breast cancer (Shu et al., 2016), glioblastoma (Cheng et al., 2013), leukemia (Mertz et al., 2011; Zuber et al., 2011), lymphoma, colon cancer (McCleland et al., 2016) and PDAC (Garcia et al., 2016; Hessmann et al., 2016; Mazur et al., 2015; Wirth et al., 2016). On the one hand, in PDAC mouse models, the tumor reduction was caused by inhibition of MYC and inflammatory signals. However, in patient-derived xenograft models, the effect of inhibiting the progression was due to the reduced CDC25B expression and therefore independent of MYC (Garcia et al., 2016; Mazur et al., 2015). Nowadays, there are several other BET inhibitors in different stages of development (Table 2). GSK 525762A (I-BET762) is tested in a phase I clinical study for solid tumors, hematologic malignancies, prostate cancer and in phase II for estrogen receptor-positive breast cancer (Stathis & Bertoni, 2018). Furthermore, a BRD2/3/4 inhibitor called OTX-015 has shown promising and stronger effects than JQ1 in cell growth inhibition, apoptosis and cell cycle arrest and is currently investigated in phase I clinical trials in PDAC, prostate cancer, hematological malignancies and prostate cancer (Pérez-Salvia & Esteller, 2017). The adverse events of OTX-015 were reported to be thrombocytopenia, anemia, gastrointestinal symptoms, fatigue and bilirubin elevation, but all of these toxic effects are reversible (Stathis & Bertoni, 2018).

In addition, BET degraders based on the PROTAC (proteolysis targeting chimeras) concept such as ARV-771, where BET inhibitors are linked to an E3 ubiquitin ligase complex to degrade the BET protein via the proteasome, have shown stronger suppression of BET protein activity and might therefore show improved antitumor activity (Stathis & Bertoni, 2018).

Table 2. BET inhibitors. *(Alqahtani et al., 2019; Raina et al., 2016; Sun et al., 2018)*

Target	Drug	Stage of clinical development
BRD2/3/4, BRDT	ABBV-075	Phase I study for solid tumors, acute myeloid leukemia, multiple myeloma, breast cancer, non-small-cell lung carcinoma
	FT-1101	Phase I study for acute myeloid leukemia
	GSK 525762A	Phase I/II study for hematological malignancies, neuroblastoma, ER-positive breast cancer, non-small-cell lung carcinoma, small-cell lung carcinoma
BRD2/3/4	OTX-015	Phase I/II study for acute myeloid / lymphoblastic leukemia, solid tumors, glioblastoma multiforme, triple-negative breast cancer, multiple myeloma
BRD2/4	GSK 2820151	Phase I study for solid tumors
BRD2	CC-90010	Phase I study for advanced solid tumors, refractory non-hodgkin lymphoma
BRD4	CPI-0610	Phase I study for lymphoma, multiple myeloma, acute myeloid / lymphoblastic leukemia, chronic myeloid leukemia
	PLX51107	Phase I study for lymphoma, solid tumors, acute myeloid leukemia
	ABBV-744	Phase I study for prostate cancer
BET-PROTAC	ARV-771	Preclinical level pan-BRD degrader in castration-resistant prostate cancer, inducing apoptosis in mantle cell lymphoma cells

Beside the toxicities, it is possible that resistance mechanism can appear to BET inhibitors. However, until now they can only be attributed to preclinical models. In PDAC, the resistance mechanism has been associated with activated Hedgehog pathway with GLI2-mediated MYC expression (Stathis & Bertoni, 2018). In contrast to this in human leukemias, MYC could be repressed by BETi, whereas the resistant ones rapidly restore the MYC transcription with activation of Wnt signaling components as a major driver to compensate the loss of BRD4 (Rathert et al., 2015).

BET inhibitors have shown synergism with various drugs in different tumor entities. The tested combinations were BETi with epigenetic inhibitors / cell cycle inhibitors / immune checkpoint inhibitors / DNA damage repair inhibitors / chemotherapeutic drugs. For instance, one of the most promising combinations were BET and PI3K inhibitors, which induced cell death and tumor regression in metastatic breast cancer (Stratikopoulos et al., 2015), as well as in ovarian, prostate and colorectal cancer cell lines (Alqahtani et al., 2019). Due to the fact that BET proteins are involved in the cell cycle, it is a logical conclusion that BETi can enhance cell cycle inhibitors. Moreover, the combination with epigenetic inhibitors such as HDAC inhibitors inducing histone hyperacetylation leads to the downregulation of MYC and BCL2 and therefore the cells become more dependent on the BET-induced transcription (Doroshow et al., 2017). One major mechanism of the tumor cells, which leads to tolerate targeted therapies via the upregulation of RKTs, could be suppressed by the inhibition of BET. In BRAF-mutant melanoma as well as in epithelial ovarian cancer BETi block the BRAFi- / MEKi-induced RTK upregulation (Kurimchak et al., 2019; Tiago et al., 2020). So, in the future there might be a possibility to prevent the establishment of resistant feedback loops via BETi.

1.7 NF-κB

Rel or NF-kappaB (NF-κB) proteins together make up together a family of transcription factors (TF) which play important roles in cellular growth and apoptosis and are continuously activated in several diseases like chronic

inflammation or cancer. Moreover, the NF-κB family has been identified as a key player in resistance mechanisms (Braeuer et al., 2006). Both subfamilies contain a Rel homology domain (RHD) for the nuclear localization and IκB inhibitor binding. RHD binds to DNA sequences known as κB sites in promoter and enhancer regions of various genes. In mammalian cells, the TF is composed of five Rel proteins: NF-κB1 (p50), NF-κB2 (p52), RelA (p65), RelB and c-Rel (Rel) that form homo- and heterodimers. The heterodimer p50-RelA is the major one in many cells. Without stimulation, the dimeric TF is bound to the inhibitor of NF-κB (IκB), its regulatory protein, which masks the nuclear localization signal of NF-κB.

Multiple pathways can lead to the activation of NF-κB signaling. The canonical (classical) pathway starts with a ligand binding to a cell surface receptor for example a toll-like-receptor, which leads to the recruitment of adaptors (TRAF) in the cytoplasm. Through TRAF the IKK complex containing the NF-κB essential modulator (NEMO) and IKKα/IKKβ is activated and consequently phosphorylates two serine residues in the IκBα regulatory domain. Consequentially, the NF-κB:IκB complex dissociates from each other and because of the exposed nuclear sequence, NF-κB is translocated into the nucleus and can bind to the κB sites. The non-canonical signaling dependent on NF-κB inducing kinase (NIK) and the activation of NF-κB induced by DNA damage via UV light via casein kinase 2 (CK2) form the other mechanisms of activation.

In cancer, elevated NF-κB activity often correlates with a poor prognosis and low sensitivity to chemotherapy in tumor cell lines because of increased cell survival and inhibition of apoptosis by stimulating the transcription of anti-apoptotic genes (Hoesel & Schmid, 2013). Although direct mutations are rare in solid malignancies, mutations of upstream signaling molecules as Ras, EGFR, PGF and HER2 can lead to continuously activation of NF-κB (Chaturvedi et al., 2011). Furthermore, some chemotherapy drugs (e.g. cisplatin) induce feedback loops that lead to translation of NF-κB target genes and therefore resistance to the cytotoxic agents. In cancer, mutations that activate the PI3K pathway are widespread and show a resistance mechanism via NF-κB because PI3K/AKT inhibitors lead to a reduction in p-AKT and NF-κB levels (Grandage et al., 2005). In addition, p53 represents another target gene of NF-κB. Therefore, the common loss-of-function p53 mutation can promote the permanent activation of NF-κB

pathway. To overcome NF-κB activity as a key player in resistance to anti-cancer agents, several targets were developed including IKK activation, IκB degradation and NF-κB DNA binding (Nakanishi & Toi, 2005). The two NF-κB inhibitors BAY 11-7082 ((E)-3-(4-methylphenylsulphonyl)-2-propenenenitrile) and BAY 11-7085 ((E)-3-[(4-*t*-butylphenyl) sulphonyl]-2-propenenitrile) inhibit the IκBα phosphorylation to sustain NF-κB in its inactivated state and have shown promising results for future combined chemotherapies. In an *in vivo* ovarian cancer model, for instance, BAY 11-7082 increased the efficacy of cisplatin (Nakanishi & Toi, 2005).

1.8 Aims of this thesis

The thesis encompasses the aim of blocking the emerging adaptive rewiring upon MTOR inhibition and understanding the underlying molecular mechanism. Based on the concept of synthetic lethality, this project aims to investigate the combinatorial effect of MTOR and BET inhibitors in murine and human PDAC cell lines for an improved targeted therapeutic option in the clinic.

2 Materials

For all experiments autoclaved pipette tips, falcons, tubes, RNase and DNase free distilled water were used.

2.1 Reagents and materials

Table 3. Reagents and materials.

Product	Manufacturer
4-Hydroxytamoxifen	Sigma-Aldrich, Steinheim
ß-Mercaptoethanol	Carl Roth, Karlsruhe
30 % Acrylamide/Bisacrylamide-stock solution (29:1)	Carl Roth, Karlsruhe
3-(4,5-dimethylthiazol-2-yl)-2,5-dipheyltetrazolium bromide	Sigma-Aldrich, Steinheim
Amersham Protran 0.2 NC Nitrocellulose Blotting membrane	GE Healthcare Life Sciences, Freiburg
Ammonium Persulfate	Sigma-Aldrich, Steinheim
Bradford reagent 5x	Serva, Heidelberg
Bromphenole Blue-Xylene Cyanole Dye solution	Sigma-Aldrich, Steinheim
BSA, Molecular Biology Grade	New England Biolabs, Ipswich, GB
Cell lysis buffer (10x)	Cell Signaling Technology, Leiden
Crystal violet	Sigma-Aldrich, Steinheim
Dimethyl Sulfoxide (DMSO)	PanReac AppliChem, Darmstadt
Disodium Phosphate Dedecanhydrate	Merck, Darmstadt
Sodium Dodecyl Sulfate	Serva, Heidelberg
dNTPs	New England Biolabs, Ipswich
Dulbecco's Modified Eagle's Medium (DMEM); high glucose	Gibco, Schwerte / Sigma-Aldrich, Steinheim
Dulbecco's Phosphate Buffered Saline	Sigma-Aldrich, Steinheim
EDTA	Gibco Schwerte
Ethanol Absolut	Otto Fischer, Saarbrücken
Ethidium bromide (EtBr)	Applichem, Darmstadt
Fetal Bovine Serum (FCS)	Sigma-Aldrich, Steinheim
Gene Ruler 100 bp DNA Ladder	Thermo Fischer Scientific, Schwerte
Giemsa	Sigma-Aldrich, Steinheim
Glycerine	Carl Roth, Karlsruhe
Glycine	Sigma-Aldrich, Steinheim
Hydrochloric acid (37 %)	Merck, Darmstadt
INK-128	LC Laboratories, Woburn, MA, USA

Isopropanol (2-Propanol)	Carl Roth, Karlsruhe
JQ1	kindly provided by Dr. Jay Bradner
Potassium chloride	Merck, Darmstadt
Methanol	Carl Roth, Karlsruhe
Magnesium Chloride	PeqLab, Erlangen
OTX-015	Medchemexpress, Monmouth Junction, NJ USA
PageRuler Prestained Protein Ladder	Thermo Scientific, Schwerte
PageRuler Plus Prestained Protein Ladder	Thermo Scientific, Schwerte
Pen Strep	Gibco, Schwerte
Phosphatase-Inhibitor-Mix	Serva, Heidelberg
Protease inhibitor cocktail tablets	Roche Diagnostics, Mannheim
Quick-Load® Purple 1 kb DNA Ladder	New England Biolabs
REDTaq® ReadyMix™ PCR reaction mix	Sigma-Aldrich, Steinheim
Skim Milk Powder	Sigma-Aldrich, Steinheim
Sodium Chloride	Serva, Heidelberg
SYBR™ Green PCR MasterMix	Thermo Fischer Scientific, Schwerte
Tetramethylenthylenediamine (TEMED)	Carl Roth, Karlsruhe
TRIS-Acetat-EDTA (TAE) (50x)	Sigma-Aldrich, Steinheim
TRIS	Carl Roth, Karlsruhe
Trypsin-EDTA solution 10x	Sigma-Aldrich, Steinheim
Tween 20	Carl Roth, Karlsruhe
Whatman Paper 3MM Chr	GE Healthcare Life Sciences, Freiburg

2.2 Cells

Table 4. Cells.

PaTu 8988t	ATTC, Manassas, VA, USA	RRID: CVCL_1847
Panc1	ATTC, Manassas, VA, USA	RRID: CVCL_0480

2.3 Antibodies

Table 5. Antibodies.

Product	Manufacturer	RRID
Anti-rabbit IgG (H+L) (Dylight® 680 Conjugate) (#5366) (1:10000)	Cell Signaling Technology, Leiden, NL	AB_10693812
Anti-rabbit IgG (H+L) (Dylight® 800 Conjugate) (#5151) (1:10000)	Cell Signaling Technology, Leiden, NL	AB_10697505
Anti-mouse IgG (H+L) (Dylight® 680 Conjugate) (#5470) (1:10000)	Cell Signaling Technology, Leiden, NL	AB_10696895
Anti-mouse IgG (H+L) (Dylight® 800 Conjugate) (#5257) (1:10000)	Cell Signaling Technology, Leiden, NL	AB_10693543
Anti-phospho-Akt (Thr308) (#2965) (1:1000)	Cell Signaling Technology, Leiden, NL	AB_2255933
Anti-phospho-p44/42 MAPK (Erk1/2) (Thr202/Tyr204) (#4370) (1:2000)	Cell Signaling Technology, Leiden, NL	AB_2315112
Anti-Akt (#9272) (1:1000)	Cell Signaling Technology, Leiden, NL	AB_329827
Anti-p44/42 MAPK (Erk1/2) (#4695) (1:1000)	Cell Signaling Technology, Leiden, NL	AB_390779
Anti-ß-Actin (#A5316) (1:1000)	Sigma Aldrich, Munich	AB_476743
c-Myc (#9402) (1:1000)	Cell Signaling Technology, Leiden, NL	AB_2151827
Anti GAPDH (ACR001PT) (1:10000)	Acris GmbH, Herford, Germany	AB_1616730

2.4 Primers

All primers were synthesized by Eurofins Genomics (Ebersberg, Germany) and diluted in H_20 to a concentration of 10 µM.

Table 6. qPCR primers.

Primer	Sequence (5'-3')
mFbxo32_qPCR_fwd	TGAGCGACCTCAGCAGTTAC
mFbxo32_qPCR_rev	TTCTCTTCTTGGCTGCGACG
mTnfaip3_qPCR_fwd	CCTGCCCAGGAGTGTTACAG
mTnfaip3_qPCR_rev	CGCGAAGTTCAGGTCCACT
mUSP11_qPCR_fwd	GCTGGCGAAAGCTGATAACAC
mUSP11_qPCR_rev	TCCTCTCCTGGCAGGCTAAT

Table 7. Primers for mycoplasm test.

Primer	Sequence (5'-3')
5´primer 1	CGC CTG AGT AGT ACG TTC GC
5´primer 2	CGC CTG AGT AGT ACG TAC GC
5´primer 3	TGC CTG GGT AGT ACA TTC GC
5´primer 4	TGC CTG AGT AGT ACA TTC GC
5´primer 5	CGC CTG AGT AGT ATG CTC GC
5´primer 6	CAC CTG AGT AGT ATG CTC GC
5´primer 7	CGC CTG GGT AGT ACA TTC GC
3´primer 1	GCG GTG TGT ACA AGA CCC GA
3´primer 2	GCG GTG TGT ACA AAA CCC GA
3´primer 3	GCG GTG TGT ACA AAC CCC GA

2.5 Devices

Table 8. Devices.

Product	Manufacturer
Analytical balance A 120 S	Sartorius AG, Göttingen
Analytical balance BP 610	Sartorius AG, Göttingen
Autoclave 2540 EL	Tuttnauer Europe B.V:, Breda, The Netherlands
Bag sealer Folio FS 3602	Severin Elektrogeräte GmbH, Sundern
Casting system gel electrophoresis Compact L/XL	Biometra GmbH, Göttingen

Centrifuge 5451R	Eppendorf, Hamburg
Centrifuge Rotina 46R	Andreas Hettich GmbH & Co. KG, Tuttlingen
CO_2 incubator MCO-5AC 17AI	Sanyo Sales & Marketing Europe GmbH, München
Electrophoresis power supply Consort EV243	Topac Inc., Cohasset, MA
Electrophoresis power supply EPS601	GE Healthcare Life Science, Freiburg
Electrophoresis power supply PowerPac 200	Bio-Rad Laboratories GmbH, München
Electrophoresis system Mini-Protean-Tetra system	Bio-Rad Laboratories GmbH, München
Electrophoretic transfer cell Mini Trans-Blot® Cell	Bio-Rad Laboratories GmbH, München
Flow Cytometer Gallios	Beckman Coulter GmbH, Krefeld, Germany
Horizontal gel electrophoresis system	Biozym Scientific GmbH, Hessisch Oldenburg
Infrared imaging system Odyssey®	LI-COR, Inc., Lincoln, NE, USA
Laminar flow HERAsafe	Heraeus Holding GmbH, Hanau
Magnetic stirrer, Ikamag® RCT	IKA® Werke GmbH & Co. KG, Staufen
Microcentrifuge 5415 D	Eppendorf AG, Hamburg
Microcentrifuge 5417 R	Eppendorf AG, Hamburg
Microplate reader Clariostar	BMG Labtech, Ortenberg
Microplate reader Multiskan RC	Thermo Labsystems, Schwerte
Microscope Axiovert 25 Inverse	Carl Zeiss, Oberkochen
Microwave	Siemens AG, München
Mini centrifuge MCF-2360	LMS Consult GmbH & Co, KG, Brigachtal
Multiple Gel Caster for SE250	Hoefer, Sulzbach
Multipette® stream	Eppendorf AG, Hamburg
pH meter 521	WTW Wissenschaftlich-Technische Werkstätten GmbH, Weilheim
Pipettes Reference®, Research®	Eppendorf AG, Hamburg
Pipetus®	Hirschmann Laborgeräte GmbH & Co. KG, Eberstadt
Real time PCR system StepOnePlus™	Applied Biosystems, Inc., Carlsbad, CA, USA
Rocking platform Biometra WT 18	Biometra GmbH, Göttingen
Scanner Epson Perfection 1200 Photo	SEIKO Epson CORPORATION, Japan
Spectrophotometer NanoDrop 1000	Peqlab Biotechnologie GmbH
Thermocycler T100	Bio-Rad Laboratories GmbH, München
Thermocycler T- Personal	Biometra GmbH, Göttingen
Thermomixer Compact	Eppendorf AG, Hamburg
UVsolo TS2 Imaging System	Analytik Jena, Jena
Vortex Genius 3	IKA® Werke GmbH & Co. KG, Staufen

Water bath 1003	GFL Gesellschaft für Labortechnik mbH, Burgwedel
Western blot system SE 250 Mighty Small II	Hoefer, Sulzbach

2.6 Kits

Table 9. Kits.

Kit	Manufacturer
Proteome Profiler™ Array Human Phospho-RTK Array Kit	R&D Systems, Inc., MN, USA
QIAshredder	Qiagen GmbH, Hilden
RNeasy Mini Kit	Qiagen GmbH, Hilden

2.7 Software

Table 10. Software.

Software	Manufacturer/website
Ascent Software 2.6	Thermo Labsystems, Schwerte
AxioVision 4.9 (RRID: SCR_002677)	Zeiss, München
CompuSyn	http://www.combosyn.com/index.html
FlowJo™ 10.4 software (RRID: SCR_008520)	FlowJo, LLC, Ashland, OR, USA
GraphPad Prism 5 (RRID: SCR_002798)	GraphPad Software, San Diego, CA, USA
Image Studio Lite version 5.2.5 (RRID: SCR_013715)	LI-COR, Inc., Lincoln, NE, USA
NCBI NucleotideBlast tool	https://blast.ncbi.nlm.nih.gov/Blast.cgi
NCBI PrimerBlast tool	https://www.ncbi.nlm.nih.gov/tools/primer-blast/
SciCrunch (RRID: SCR_003115)	https://scicrunch.org/resources
StepOne™ Software (RRID: SCR_014281)	Applied Biosystems, Inc., Carlsbad, CA, USA
SynergyFinder (RRID: SCR_019318)	https://synergyfinder.fimm.fi
SynLethDB (accessed 11/2018)	http://histone.sce.ntu.edu.sg/SynLethDB/

2.8 Media/Buffers/Solutions

Table 11. Overview of all used media, buffers and solutions.

Medium/Buffer/Solution	Composition
Agarosegel (1.5 %)	400 ml 1x TAE
	6 g Agarose
	0.00625 % (v/v) EtBr
Crystal violet dye solution	2 % EtOH
	0.2 % Crystal violet
Dulbecco's Modified Eagles Medium, high glucose (supplemented with FCS and Pen Strep)	10 % (v/v) FCS
	1 % (v/v) penicillin/streptomycin (Pen Strep)
Freezing medium	Dulbecco's Modified Eagles Medium, high glucose
	20 % (v/v) FCS
	10 % (v/v) DMSO
KCM buffer (5x)	2 M KCl
	1 M $CaCl_2$
	1 M $MgCl_2$
Laemmli (5x)	0.3 M TRIS
	50 % (v/v) Glycerine
	0.35 M SDS (pH 6.8)
	0.05 % Bromophenol blue
	5 % (v/v) ß-Mercaptoethanol
Running buffer (1x)	192 mM Glycine
	25 mM TRIS
	3.47 mM SDS
PBS (1x), pH 7.4	137 mM Sodium chloride
	270 µM Kalium chloride
	4.02 nM Disodium phosphate
PreMix (PCR)	1x Buffer S
	6 % Sucruose
	20 % SucRed
	0.4 µM dNTP
	Each 60 U/ml Taq DNA Polymerase (Peqlab)
RIPA buffer	50 mM TRIS-HCl
	150 mM NaCl
	2 mM EDTA
	1 % Triton X100
	1 % Sodium deoxycholate
	0.1 % SDS
TAE buffer (1x), pH 7.6	1 mM EDTA
	40 nM TRIS
	20 mM acetic acid
Transfer buffer (1x)	192 mM Glycine
	25 mM TRIS
	20 % (v/v) Methanol

Stacking gel (4.5 %)	125 mM TRIS-HCl, pH 6.8
	4.5 % (v/v) Acrylamide
	0.1 % (v/v) SDS
	0.05 % (w/v) APS
	0.2 % (v/v) TEMED
Separation gel (10 %)	390 mM TRIS-HCl, pH 8.8
	10 % (v/v) Acrylamide
	0.1 % (v/v) SDS
	0.05 % (w/v) APS
	0.15 % (v/v) TEMED
Separation gel (15 %)	390 mM TRIS-HCl, pH 8.8
	15 % (v/v) Acrylamide
	0.1 % (v/v) SDS
	0.05 % (w/v) APS
	0.15 % (v/v) TEMED

3 Methods

The experiments were performed according to the manufacturer's protocol if not stated different.

3.1 Cell culture

All cell culture experiments were performed in a laminar flow bench under sterile conditions and cells were cultivated at 37°C and 5 % CO_2 in suitable media (Table 11). As part of this thesis, several murine pancreatic cancer cell lines were used whose identity was verified by using genotyping PCR. The two utilized human PDAC cell lines (PaTu 8988t, Panc1) were authenticated by single-nucleotide polymorphism (SNP) profiling conducted by Multiplexion (Multiplexion GmbH, Heidelberg, Germany). For detection of Mycoplasma contamination, the cell lines were tested by a PCR-based method described by Ossewaarde et al. (1996).

3.2 Handling and cryopreservation of pancreatic tumor cells

The murine and human PDAC cells were regularly supplied with fresh, pre-warmed media with 10 % FCS (fetal calf serum). When the cell lines reached approximately 80 % confluence, the cells were passaged. For passaging, the PDAC cells were washed with PBS (phosphate buffered saline), detached with Trypsin for 5 min at 37°C and split into a new flask with fresh medium. For determining the cell number, a Neubauer counting chamber, was used.

For the long-term storage: after trypsinization, the cells were resuspended in fresh medium and centrifuged at 200 x g at 4°C for 5 min. In the following step, the supernatant was discharged and the cell pellet was resuspended in ice-cold freezing medium and pipetted in 1 ml aliquots in cyrotubes. For a few days the cells were stored at -80°C then transferred to liquid nitrogen.

3.3 MTT assay

MTT assay is a metabolic assay used for measuring the viability of the cells (Mosmann, 1983). Viable cells can convert the yellow tetrazolium MTT (3-(4,5-dimethylthiazol-2-yl-)-2,5-diphenyltetrazolium bromide) to a purple formazan product by mitochondrial reductase enzymes. The formazan crystals can be dissolved and the resulting colored solution measured in a spectrophotometer.

Dependent on their growth properties, 3000 - 5000 cells per well were seeded in triplicate into a 96-well microplate in 100 µl medium. The cells were allowed to attach overnight and treated on the next day with INK-128 (MTOR inhibitor), VEGFR- (SAR131675, Axitinib), Axl- (Gliterinib), NF-κB- (IKK-16, BAY11-7085, BAY11-7082), BET inhibitors (JQ1, OTX-015, GSK525762A), BET-PROTAC (ARV-771) and their combination. After 72 hours, 10 µl of MTT reagent (5 mg/ml MTT in PBS) was added to each well and the plates were incubated at 37°C for 4 h. Afterwards, the medium was carefully removed and 200 µl of DMSO:EtOH (1:1) was added for lysing the colored cells. The plates were then incubated at RT on the shaker for 15 min, before determining the absorbance at 595 nm wavelength with the plate reader Multiskan RC from Thermo Labsystems. Three biological replicates in independent experiments were performed and analyzed.

3.4 Clonogenic assay quantification

The Clonogenic assay is a long-term growth assay that determines the ability of single cells to form colonies. In 1956, it was first published by Puck and Marcus (Puck & Marcus, 1956), who demonstrated the effect of x-rays on mammalian cells by measuring their colony-forming ability. Here, it was used to determine the long-term growth inhibitory effect of drugs or drug combinations on different PDAC cell lines.

In order to quantify the long-term growth of the cells in the Clonogenic assay, cells were stained with Crystal Violet, which allows for solubilization of the dye and subsequent absorbance measurement.

For the Clonogenic assay with Crystal Violet, which stains DNA, 1000 - 2000 cells were seeded (dependent on the proliferation rate of the different cell lines) in 12-/24-well plates in 1 ml or 0.5 ml medium respectively. After incubating the cells overnight at 37°C to enable adhesion of the cells to the wells, the single drugs or combinations were supplemented. When the cells in the vehicle-treated (DMSO) control well nearly reached confluence, the medium was carefully removed from the wells, washed with PBS and stained with 0.2 % crystal violet solution for 10 minutes on a shaker at room temperature. To remove unspecific background staining, the wells were washed two times with distilled water. The plates were then imaged on an Epson Perfection 1200 Photo scanner for documentation. Afterwards the plates were drained upside down and then 1 % SDS was added to solubilize the stain. Before measuring, the plates were put on a shaker until the color was uniform. Because of the solubilization the amount of taken up dye can be quantified by measuring the absorbance of each well at 570 nm with the Clariostar microplate reader from BMG Labtech.

3.5 PCR for mycoplasm test

Before performing the mycoplasm test, the cells were cultivated at least one week without Pen Strep in a 10 cm dish until the cells were almost confluent. Two ml of the supernatant were taken and centrifuged for 2 min at 250 x g followed by transferring the supernatant to a new reaction vessel and centrifuged again for 10 min at 16000 x g. Afterwards, the pellet was resuspended in 50 µl PBS and heat inactivated at 95°C for 3 min. As the DNA template was finished, the PCR mix was prepared (Table 12) and the PCR cycles were started (Table 13).

Table 12. PCR mix with RedTaq.

Reagents	Volume [µl]
Premix	15
10 µM Primer Forward	2
10 µM Primer Reverse	2
Template	2
Deionized H_2O	9

Table 13. Thermocycling conditions for PCR.

PCR program	Temperature	Time
Initial cell lysis and denaturation	95°C	15 min
40 cycles	94°C	1 min
	60°C	1 min
	74°C	1 min
Final amplification	72°C	10 min
Pause	25°C	∞

Finally, in the electrophoresis chamber, a 1.5 % agarose gel containing 0.2 µg/ml Ethidium bromide covered with 1x TAE buffer was loaded with 5 µl PCR product and 25 µl GeneRuler DNA ladder. After running the gel for 1.5 - 2 hours at 120 V, the UVsolo TS imaging system was used to visualize the DNA fragments. To verify the PCR results, one positive and negative control were included.

3.6 Molecular techniques

3.6.1 RNA analysis

3.6.1.1 RNA isolation

First, for isolating the RNA, the medium was aspirated and the plates washed once with PBS. Harvesting with 600 µl (for 10 cm dish) lysis buffer (RLT) and 2-Mercaptoethanol (1:100) was done on ice to prevent RNA degradation until further processing the lysates were stored at -80°C. Next, for purifying the RNA the RNeasy mini kit (Qiagen) was used according to the manufacturer's instruction. The samples were diluted with 70 % ethanol (1:1), bound to the column and once washed with wash buffer. To avoid contamination of the lysates with genomic DNA the on-column DNase digestion was performed, incubating the samples for 15 min at room temperature. The following step was again washing the lysates with wash buffer and eluted with RNase-free water. The RNA concentration was measured with the NanoDrop 1000 spectrophotometer and the isolated RNA was stored at -80°C until further use.

3.6.1.2 Reverse transcription

For the reverse transcription (RT) to generate the cDNA (100 µl), 2 µg RNA (38,5 µl) and the TaqMan RT reagents (61,5 µl per reaction) were used. After adding the MasterMix (Table 14) to the diluted RNA, RT was performed in a PCR-cycler according to the described conditions (Table 15). Until further use, the produced cDNA was stored at -20°C.

Table 14. Reverse transcription reagents MasterMix (TaqMan RT).

Reagents	Final concentration	Volume per 1x reaction [µl]
10x buffer	1x	10
$MgCl_2$ (25 mM)	5.5 mM	22
dNTP-Mix (10 mM)	500 µM each	20
Random hexamers	2.5 µM	5
RNase Inhibitor	0.4 U/µl	2
MultiScribe RT (50 U/µl)	1.25 U/µl	2.5

Table 15. Conditions for RT PCR.

Temperature	Time
25°C	10 min
48°C	1 h
95°C	5 min
4°C	Pause

3.6.1.3 Quantitative real-time PCR

The primers (Table 6) were designed with the NCBI Primer-BLAST tool (Ye et al., 2012) (Table 10) and before using tested for their efficiency. Therefore, serial dilutions of cDNA were tested and the C_T (cycle threshold) values vs. the log cDNA concentration were blotted to calculate the slope (slope -3.322 = amplification factor 2 = 100 % efficiency). Only primers with efficiency of at least 90 % were used. For performing the real-time PCR with the StepOnePlus real-time PCR system and software (Table 17) the “Power SYBR Green PCR MasterMix” (Table 16) and 100 nM of the forward and the reverse primer were used. The pipetting was performed on ice to prevent the degradation of the cDNA.

The samples were normalized to ß-actin as a housekeeping gene and exerted in three technical triplicates in three independent experiments. The results were analyzed by the $\Delta\Delta C_T$ method (Pfaffl, 2001) for the relative quantification.

$\Delta C_T = C_T$ (target gene) - C_T (endogenous control)

$\Delta\Delta C_T = \Delta C_T$ (treated sample) - ΔC_T (reference sample)

Relative expression = $2^{-\Delta\Delta C_T}$

Table 16. Power SYBR Green PCR MasterMix.

Reagents	Volume per 1x reaction [µl]
2x SYBR MM Buffer	6.25
Forward primer	0.125
Reverse primer	0.125
Deionized H_2O	3.5

Table 17. Conditions for quantitative real-time PCR.

Temperature	Time	Numbers of cycles
50°C	2 min	1
95°C	10 min	1
95°C	15 sec	40
60°C	1 min	40

3.6.1.4 RNA-sequencing (RNA-Seq)

For the RNA-sequencing (RNA-Seq) the mRNA was extracted in the same way as described above and further analyzed on a NextSeq 500 (Illumina) system by Dr. Rupert Öllinger (in the lab of Prof. Dr. Roland Rad, TranslaTUM, Technical University Munich). Before sequencing, the library preparation for bulk-sequencing was performed as previously described (Parekh et al., 2016). The barcoded cDNA was generated with a Maxima RT polymerase (Thermo Fisher) by using oligo-dT primer containing barcodes, unique molecular identifiers (UMIs) and an adaptor. For extending the 5'ends of the cDNA a template switch oligo was used and with primers binding to the template switch oligo and adaptor, the cDNA was amplified. After the cDNA fragmentation and ligation of the TruSeq

adapters with the NEBNext® Ultra™ II FS DNA Library Prep Kit (Illumina), the 3'end fragments were amplified using primers with Illumina P5 and P7 overhangs. The P5 and P7 sites were exchanged compared to Parekh et al. (2016) to achieve a better cluster recognition. In read1 the cDNA with 65 cycles and the barcodes and UMIs with 16 cycles in read2 were sequenced on the NextSeq 500 (Illumina). Finally with the published Drop-seq pipeline (v1.0) the data was processed to generate sample- and gene-wise UMI tables (Macosko et al., 2015).

Further the demultiplexed data was analyzed by PD Dr. rer. nat. Matthias Wirth (Charité-Universitätsmedizin Berlin, Campus Benjamin Franklin). The resulting Fastq files were processed and analyzed with the Galaxy platform (Afgan et al., 2016; Goecks et al., 2013). Briefly, count tables were normalized with Deseq2 and resulting differential gene expression tables (rLog) were used for further analyses. Next, the gene set enrichment analysis (GSEA) tool (Subramanian et al., 2005) was used. mRNA expression of MTORi, BETi and combined MTORi + BETi treated cells can be accessed via: PRJEB47050. In the figure, the nominal P-value and false discovery rate (FDR) q-value are indicated.

3.6.2 Protein analysis

3.6.2.1 Isolation of the whole cell protein extract

For collecting the whole cell lysate, the plates were washed with ice-cold PBS and lysed in RIPA buffer with freshly added protease and phosphatase inhibitors. Afterwards, the samples were centrifuged in a precooled centrifuge for 20 min at 4°C and the supernatant transferred to new tubes. The lysates were stored at -80°C for further use.

3.6.2.2 Bradford protein assay

For measuring the protein concentration according to Bradford (Bradford, 1976), 300 µl Bradford reagent was pipetted in a 96-well plate and 1 µl of the protein lysate was added. The assay was performed in triplicates and defined dilutions

of bovine serum albumin (BSA) were used as a standard curve. The dye Coomassie Brilliant Blue G-250 binds to the proteins in acidic solution that results in a color change, which causes a shift in the absorbance maximum from 465 nm to 595 nm. The increase of absorbance at 595 nm is detected with the Multiskan RC plate reader (Thermo Labsystems). By adding RIPA buffer and 5x-Laemmli-buffer, the protein samples were adjusted to equal concentration and then incubated for 5 min at 95°C. Until further use, the extracts were stored at -20°C.

3.6.2.3 Western immunoblot

This technique is used to separate the proteins according to their molecular weight, label, visualize and quantify them after incubating with specific antibodies for the proteins of interest.

The separating gel solution (appropriate gel acrylamide percentage based on the protein size) was mixed according to the protocol, added to the gel rack for solidification, covered with isopropanol to obtain a straight gel line and polymerized for 20 min. After discharging the isopropanol, the stacking gel was mixed, added on top of the separating gel and a comb was inserted to create the wells. The rack was placed in an electrophoresis chamber and covered with running buffer. Then the protein samples (100 - 120 µg) were loaded into each well followed by the PageRuler protein marker for determining the protein size. The gels were run at 80 - 120 V for 2 - 3 hours (until the dye front disappeared from the gels).

For the transfer, the chambers were filled with cold 1x transfer buffer, an ice pack and surrounded by ice for cooling. The gels, nitrocellulose membranes and Whatman filter papers were wetted before further use. Afterwards, the transfer sandwich (3 Whatman filter paper – gel – membrane – 3 Whatman filter paper) was created and placed in the cassette with the gel next to the cathode and the membrane near the anode in the chamber. The transfer was performed at 100 V and 350 mA (for one transfer chamber; 170 V and 350 mA for two chambers) for 2 hours.

The membranes were blocked with 5 % skim milk in PBS for 1 hour to minimize the unspecific antibody binding followed by washing with 0.1 % Tween in PBS for

5 min and incubated with a primary antibody overnight at 4°C. Before the incubation with the secondary antibody for 1 hour at room temperature the membranes were washed with 0.1 % Tween in PBS 3 times for each 5 min. This washing step was repeated after the incubation with the secondary antibody. Afterwards, to visualize the protein bands the membranes were scanned at 700 or 800 nm depending on the used secondary antibody.

Image Studio Lite version 5.2.5 was used to quantify the scanned membranes.

3.6.2.4 Phospho-receptor tyrosine kinase (RTK) array

The human Phospho-RTK Array Kit (Proteome Profiler™; R&D Systems, Inc., MN, USA) was used to detect changes in the phosphorylation of RTKs after treatment with MTOR inhibitor. On one nitrocellulose membrane, 49 different phosphorylated RTKs (antibodies and controls are spotted in duplicate) can be screened.

The RTK Array was performed according to the manufacturer's instructions. Briefly, the cells were harvested and resuspended in the provided Lysis Buffer 17 (prepared with protease and phosphatase inhibitor). To prepare the membranes, they were blocked with Array Buffer 1 for 1 hour. Meanwhile, the samples were centrifuged in a precooled microcentrifuge for 5 min. The membranes were covered with the sample lysates (diluted with Array Buffer 1 to 1.5 ml) on a shaker at 4°C overnight. Following washing the membranes 3 times for 10 min with 1x Wash Buffer, incubation with the Anti-Phospho-Tyrosin- HRP Detection Antibody on a shaker at room temperature for 2 hours was performed. Prior to the incubation with the Chemi Reagent Mix for 1 min, the washing steps were repeated as described before. To visualize the chemiluminescent signal the membranes were scanned with the Odyssey from LI-COR.

For the quantification, Image Studio Lite version 5.2.5 was used.

3.6.3 Cell cycle analysis

The cell cycle profile was determined by staining DNA with propidium iodide (PI) and measuring its intensity. The analysis is based on the quantitation of DNA content that is stoichiometrically stained with PI. Ideally, one single cell is passing the laser beam and due to the dye, the differentiation of the cells in subG1-, G1-, S- and G2-phase is possible.

For harvesting the cells, the used medium was collected in a 15 ml centrifuge tube, the attached cells were washed with PBS, dissociated with trypsin and added to the tube with the medium. The samples were centrifuged for 5 min at 4°C with 210 x g, followed by removing the supernatant. To allow the entry of the dye, the cells were fixated with 1 ml 70 % ethanol at 4°C overnight. After the fixation, 1 ml ice-cold PBS was added and the samples were centrifuged again for 5 min at 4°C with 210 x g. The supernatant was removed and the pellet resuspended in 1 ml PBS. To avoid the staining of RNA, RNase (final concentration 50 µg/ml) was added and incubated with the samples for 1 h at 37°C in the dark. Prior to measuring the samples with the Gallios flow cytometer (Beckman Coulter) the PI (final concentration 50 µg/ml) was added. The results were analyzed with the FlowJo^{TM} 10.4 software.

3.6.4 Statistical analysis

Statistical analysis was performed with GraphPad Prism 5. For the statistical significance the ANOVA or the two-sided Student's t-test was used. P values were calculated by using GraphPad Prism 5 and are indicated within the figure legends. As significance levels error probability p was employed ($p<0.05$ (*), $p<0.005$ (**), $p<0.001$ (***)). All data determined from at least three independent experiments (otherwise stated in the figure legends) and presented as mean and standard deviation (SD).

4 Results

4.1 RTK activation upon inactivation of MTOR

One main aim of this thesis was to investigate the mechanism of the adaptive rewiring, resulting in the hyper-activation of two main driver pathways in PDAC (ERK and PI3K signaling pathway) after genetic or pharmacological blockage of MTOR (Hassan et al., 2018).

The Human Phospho-RTK Array Kit was used to determine the tyrosine phosphorylation of 49 different human RTKs in an unbiased manner. After blocking MTOR pharmacologically over 72 h with 500 nM INK-128 (replacing medium with inhibitor every 24 h), phosphorylation of several RTKs such as VEGFR3, IR, IGF1R and AXL was increased (Figure 2A and Figure 2B). In order to determine whether the activated RTKs have a functional role in limiting the cellular response towards MTORi, cell viability assays with different VEGFR- and AXL-inhibitors were performed. Two VEGFR inhibitors were applied: SAR131675 more selective for VEGFR3 than VEGFR1/2 and Axitinib a multi-target inhibitor against VEGFR1, -2, -3. The expectation was that SAR131675, Axitinib or Gilteritinib (AXL inhibitor) should function synergistically in combination with the MTOR inhibitor (MTORi) INK-128 if these RTKs are involved in the acquired resistance of the PDAC cells. As shown in the dose-response curves (Figure 2C - E), only between INK-128 and Gilteritinib (Figure 2E) a left shift in the dose-response could be determined. To validate the synergism between the different inhibitors, the combination index values were calculated using CompuSyn. CI-values below 1 represent synergism, meaning the effect of both drugs is higher than expected, while CI-values higher than 1 are antagonistic, indicating that the combination is less effective than the sum of the two individual drugs. CI-values equal to 1 indicate an additive effect of the two drugs according to the definition from Chou and Talalay (Chou & Talalay, 1984). The CI values for the combination treatment of INK-128 and Gilteritinib in a human (PaTu 8988t) and a murine (murine genotype: *Ptf1a*$^{Cre/+}$*; LSL-Kras*$^{G12D/+}$*) (*53631ppt) PDAC cell line is illustrated in the heatmap in Figure 2F, showing synergism over a wide dose-range for the human PDAC cell line. No synergism was found in the murine line for the combination of MTORi and AXLi as the CI values were higher than 1 for the majority of dose combinations. Due to the heterogeneity in the observed

synergism (Supplemental Figure 1) RTKs were not followed further in the current work.

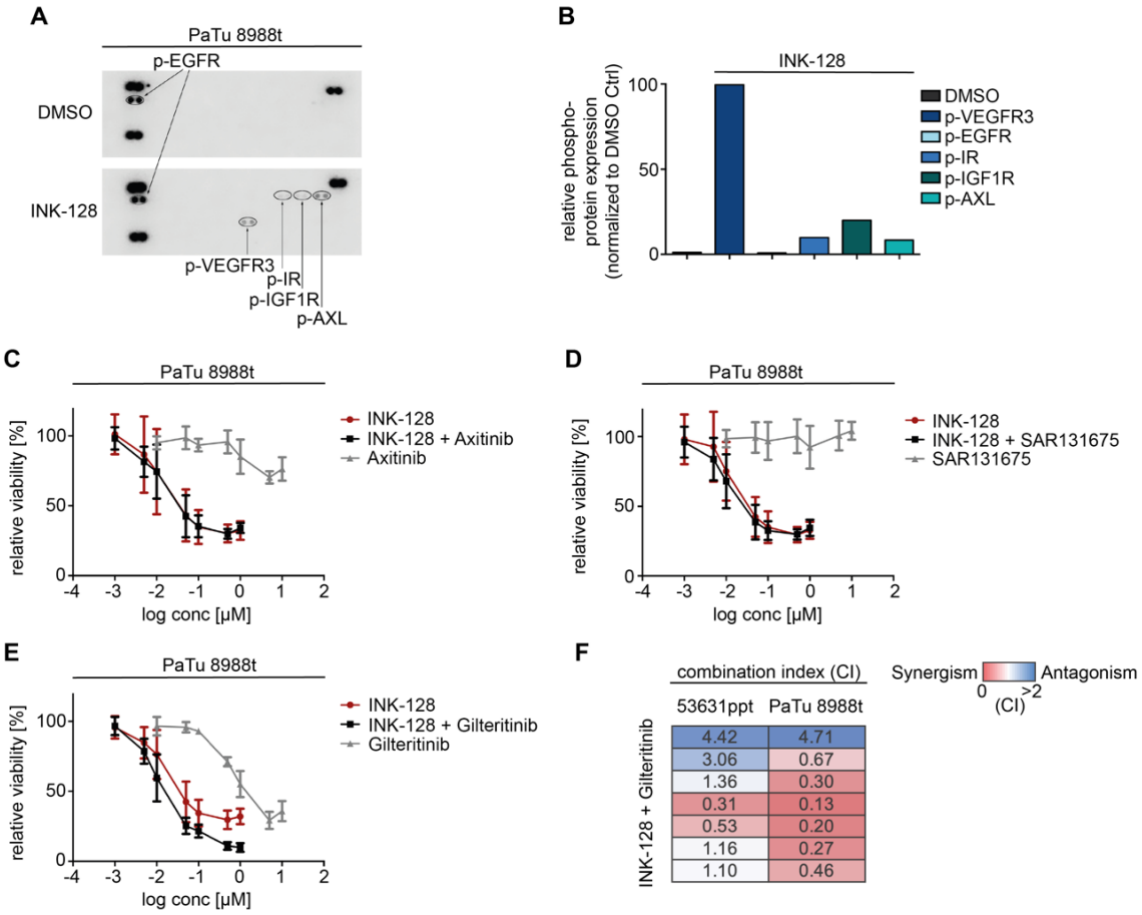

Figure 2. RTK activation upon inactivation of MTOR.

(A) RTK-Array with activated p-VEGFR3, p-IR, p-IGF1R and p-AXL after INK-128 (500 nM) treatment for 72 h. Medium with fresh drug was replaced every 24 h. (n=1) (B) Quantification of the RTK-Array (normalized to DMSO treated control) as described in (A). (C) – (E) The indicated human PDAC cell line was treated with INK-128 (1 – 1000 nM), Axitinib/Gilteritinib/SAR131675 (0.01 - 10 µM) or in combination therapies (n=4, except Gilteritinib n=3). After 72 h the viability was measured in MTT assays. (F) Heatmap showing calculated CI values for Gilteritinib with one murine and one human cell line.

4.2 Addressing upregulation of NF-κB pathways upon MTOR blockage

To identify further pathways that might play a role in the acquired resistance to the inhibition of MTOR, recently published RNA-Seq data were analyzed by a Gene Set Enrichment Analysis (GSEA). The dataset was from a murine PDAC cell line PPT-ZH363-*Mtor*$^{\Delta E3/lox}$ (Hassan et al., 2018), which allows Cre-mediated genetic deletion of MTOR. An activation of a gene signature linked to the TNFα (tumor necrosis factor alpha)/NF-κB signaling pathway (Figure 3A) was observed, pointing to an alternative pathway ensuring cellular survival upon MTOR knockout. To validate the findings (Figure 3B), three of the top upregulated NF-κB target genes, A20 (TNFAIP3), FBXO32 and USP11 were further validated. Therefore, murine 53631ppt PDAC cells were treated for 24 hours with 500 nM INK-128. Quantitative real-time PCR demonstrated a significant upregulation of all three genes (Figure 3C - E), thus confirming on a pharmacological level the previous RNA-Seq results from the genetic model.

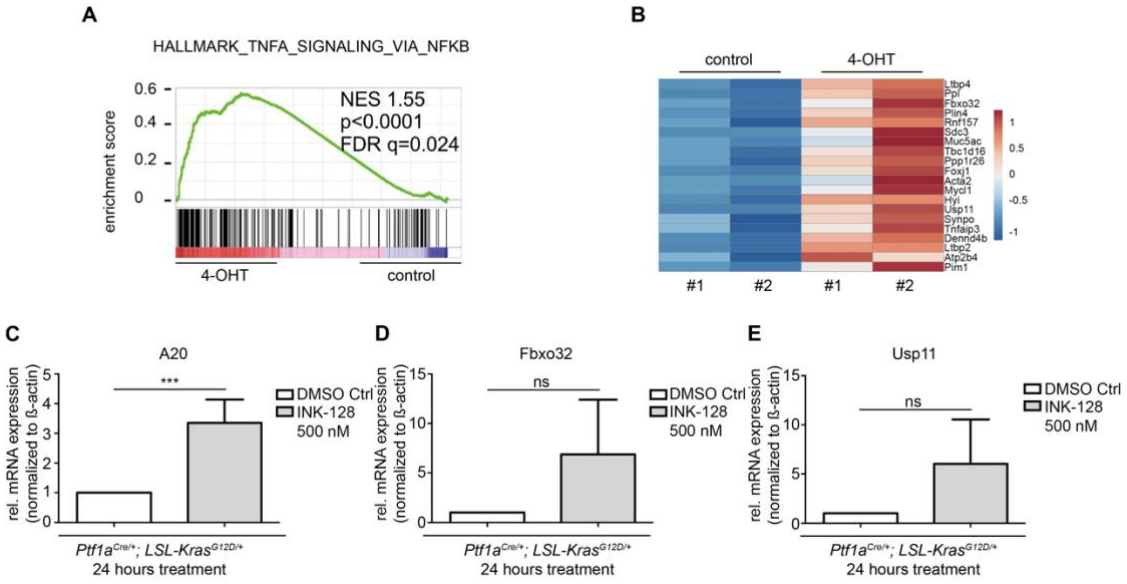

Figure 3. Upregulated TNFα/NF-κB signaling upon MTOR knockout.

(A) PPT-ZH363-Mtor$^{\Delta E3/lox}$ *cells were treated with 4-OHT (600 nM) over 8 days to delete MTOR. Afterwards, mRNA expression was profiled using RNA-Seq and analyzed by GSEA. The normalized enrichment score (NES), nominal P-value, FDR q-value are indicated. (B)*

*Heatmap of the top 20 upregulated genes involved in TNFα/NF-κB signaling upon 4-OHT treatment. (C) – (E) Ptf1a$^{Cre/+}$; LSL-Kras$^{G12D/+}$ cells were treated with INK-128 for 24 hours. mRNA expression of A20, Fbxo32 and Usp11 was determined by qPCR using ß-actin mRNA expression as reference (n=3; A20: n=5). ***P-value of an unpaired Student's t-test =0.0002.*

To determine whether the observed upregulation of NF-κB signaling had any functional relevance towards cellular viability and survival and whether this could be addressed therapeutically, three different IKK inhibitors were examined. IKK-16, an IκB kinase inhibitor for IKK-2, IKK complex and IKK-1 was used in combination with INK-128. In addition to IKK-16, BAY11-7085 and BAY11-7082 (0.1 - 100 µM), both inhibiting the TNFα-induced IkBα phosphorylation were studied to investigate their effect towards the cell viability by MTT (Figure 4A - C). To determine the synergism between the MTOR- and IKK-inhibitors, the CI-values were calculated again using CompuSyn for one murine (53631ppt) and one human (PaTu 8988t) cell line. While for some of the tested dose combinations, a slight synergism was observed, the majority of combinations showed CI-values above 1 indicating that overall, there does not seem to be a synergistic benefit by combining MTOR- and IKK-inhibitors (Figure 4D - F).

These findings were validated with clonogenic assays, a long-term cell viability assay (Figure 4G) (Supplemental Figure 2). SynergyFinder (Ianevski et al., 2017) was utilized to determine the synergism according to the zero interaction potency (ZIP) model (Yadav et al., 2015) between IKK-16 and INK-128. While the isobologramm (Figure 4H) demonstrates two synergistic peaks (in red) in the combination matrix, large parts are non-synergistic and the overall synergy score (3.167) is quite low.

Besides verifying this on pharmacological level, RelA-pro- and deficient clones (Conradt et al., 2013) were examined upon MTOR blockage. In the MTT viability assay, no significant change towards the RelA deficiency was displayed (Supplemental Figure 6).

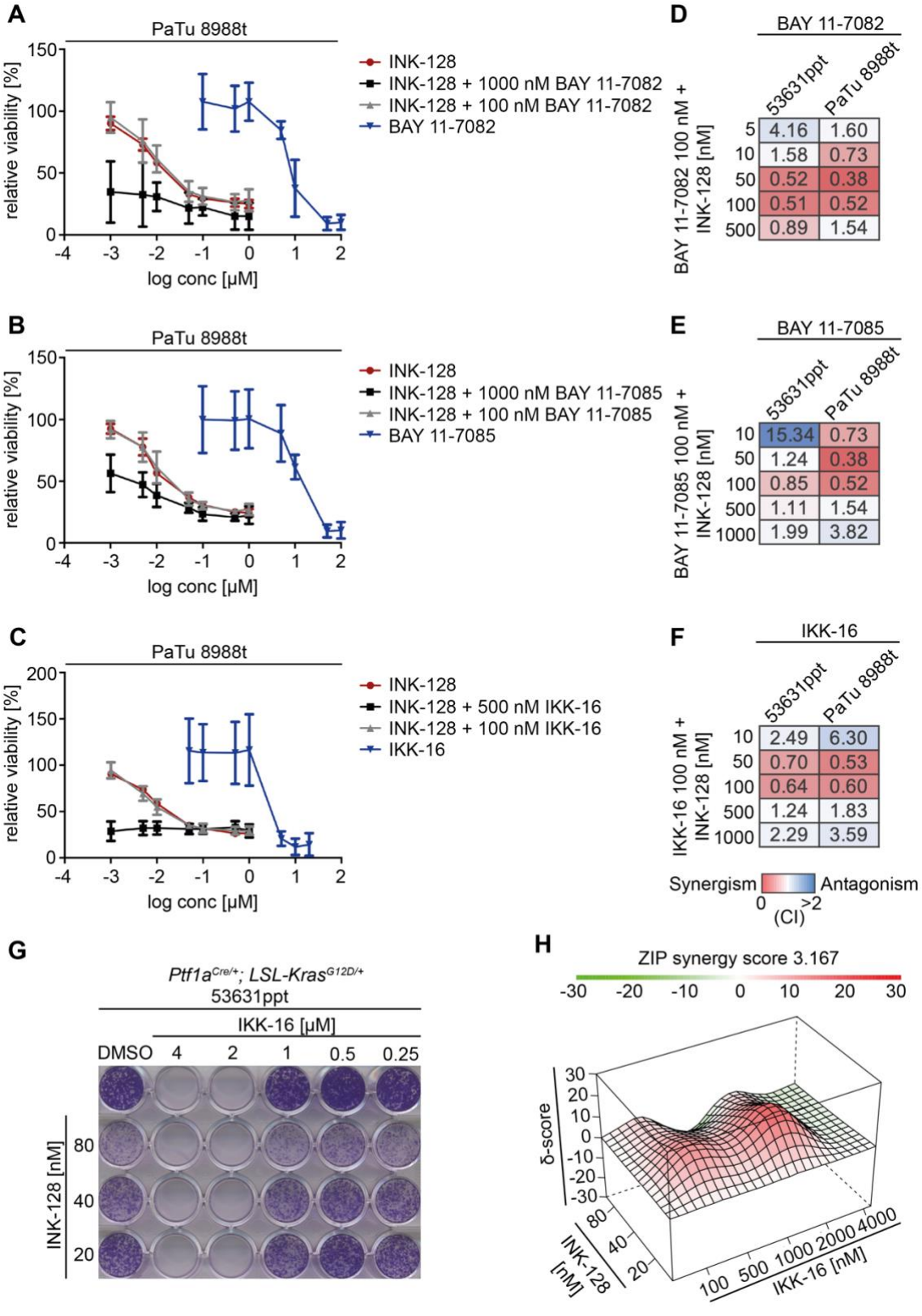

Figure 4. Addressing upregulated NF-κB signaling with different IKK inhibitors.

(A) – (C) The PaTu 8988t cells were treated with INK-128, BAY 11-7082/BAY 11-7085/IKK-16 or in combination therapies. After 72 h the viability was measured in MTT assays (n=3). (D) – (F) Heatmap with calculated CI values for the corresponding drugs on the left with one murine and one human PDAC cell line. (G) Exemplary clonogenic assay performed as a

long-term viability assay with the indicated drug treatment. (H) Isobologramm depicting the adjacent scan. 3D representation from SynergyFinder displays the synergistic (red) and antagonistic (green) areas across the entire matrix.

4.3 MTOR-deficiency linked to an increased BET inhibitor sensitivity

In order to identify molecular targets whose inhibition might work synthetically lethal in conjunction with MTOR inhibition, SynLethDB (Guo et al., 2016), a comprehensive database of synthetic lethality (SL) pairs was accessed to identify genes that are predicted to have a synergistic effect upon MTOR inhibition (Figure 5A). The top MTOR SL partners shown in Figure 5B according to their confidence score (CS) were VHL (Von Hippel-Lindau tumor suppressor) (CS=0.86), PTEN (phosphatase and tensin homolog) (CS=0.9) and MYC (CS=0.76). As VHL has an unknown role in PDAC and is difficult to target, just as PTEN, which acts upstream in the same signaling pathway as MTOR, the focus was to target MYC. While MYC itself is still considered to be undruggable, it is possible to indirectly target it by the BRD4 pathway using BET inhibitors (BETi) such as JQ1 or OTX-015 (Delmore et al., 2011).

To validate the SL concept, the BET inhibitors were tested in MTOR deficient (n=3) versus MTOR proficient (n=4) clones from the aforementioned murine PDAC cell line PPT-ZH363-Mtor$^{\Delta E3/lox}$. Assays were performed by clonogenic growth assays with two different concentrations of each inhibitor. Colony formation upon treatment with JQ1 (Figure 5C) or OTX-015 (Figure 5D) in the MTOR-deficient cell clones were significantly reduced compared to MTOR-proficient clones, demonstrating that MTOR-deficiency seems to be linked to an increased BETi sensitivity.

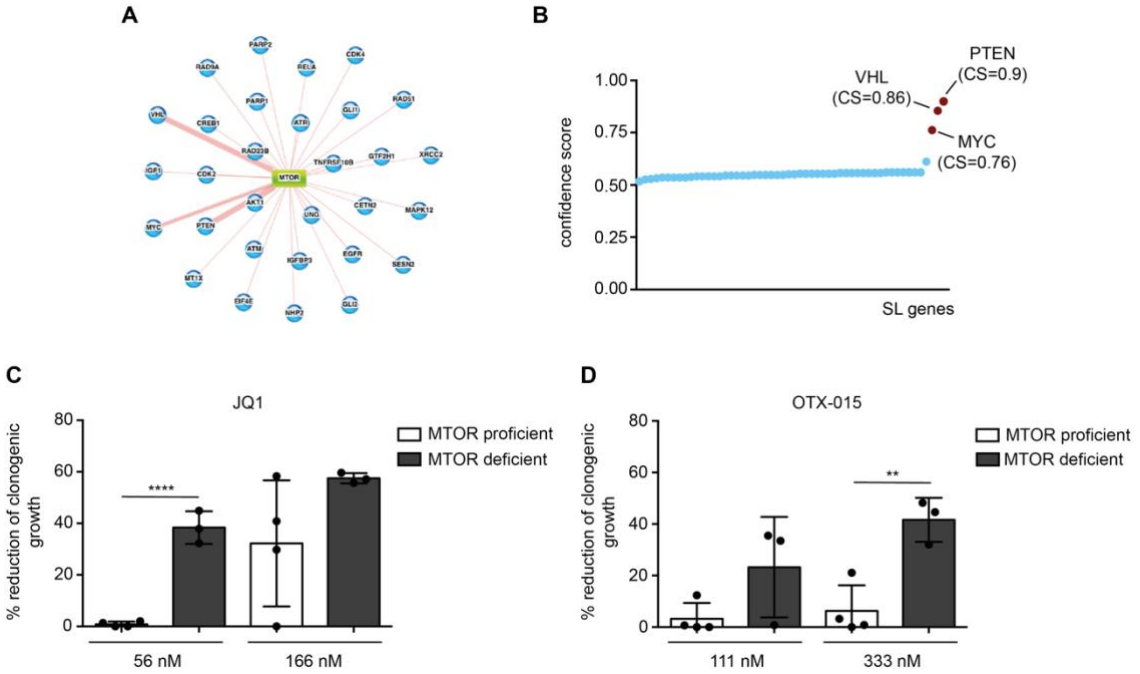

Figure 5. MTOR-deficiency linked to an increased BET inhibitor sensitivity.

*(A) Network view of all SL pairs for MTOR collected by SynLethDB. (B) MTOR-centered SL genes with PTEN (CS=0.9), VHL (CS=0.86) and MYC (CS=0.76). Confidence score close to 1 represents higher confidence. (C) Quantification of clonogenic assays from 4 Mtor-proficient and 3 -deficient clones after JQ1 treatment (n=1). ****P-value of an unpaired Student's t-test <0.0001. (D) Quantification of clonogenic assay from 4 Mtor-proficient and 3 -deficient clones after OTX-015 treatment (n=1). **P-value of an unpaired Student's t-test =0.0044.*

4.4 MTOR-based combination therapies with different BET inhibitors

To determine whether combined inhibition of MTOR and BET proteins might be a therapeutic option in PDAC, different BETi were tested in murine and human PDAC cell lines in combination with the MTOR inhibitor INK-128. MTT and clonogenic growth assays were used to determine the synergism between MTOR and BET inhibitors.

A left shift in the dose-response could be observed in the combination treatment compared to single inhibitor treatments in MTT assays across different murine and human cell lines (Figure 6A - D) as well as with different BET inhibitors such as GSK525762A (Figure 6A), JQ1 (Figure 6B), ARV-771 (Figure 6C) and OTX-

015 (Figure 6D). This synergistic effect was also observed in long-term clonogenic assays as depicted in Figure 6E (Supplemental Figure 3; Supplemental Figure 4) and Figure 6F.

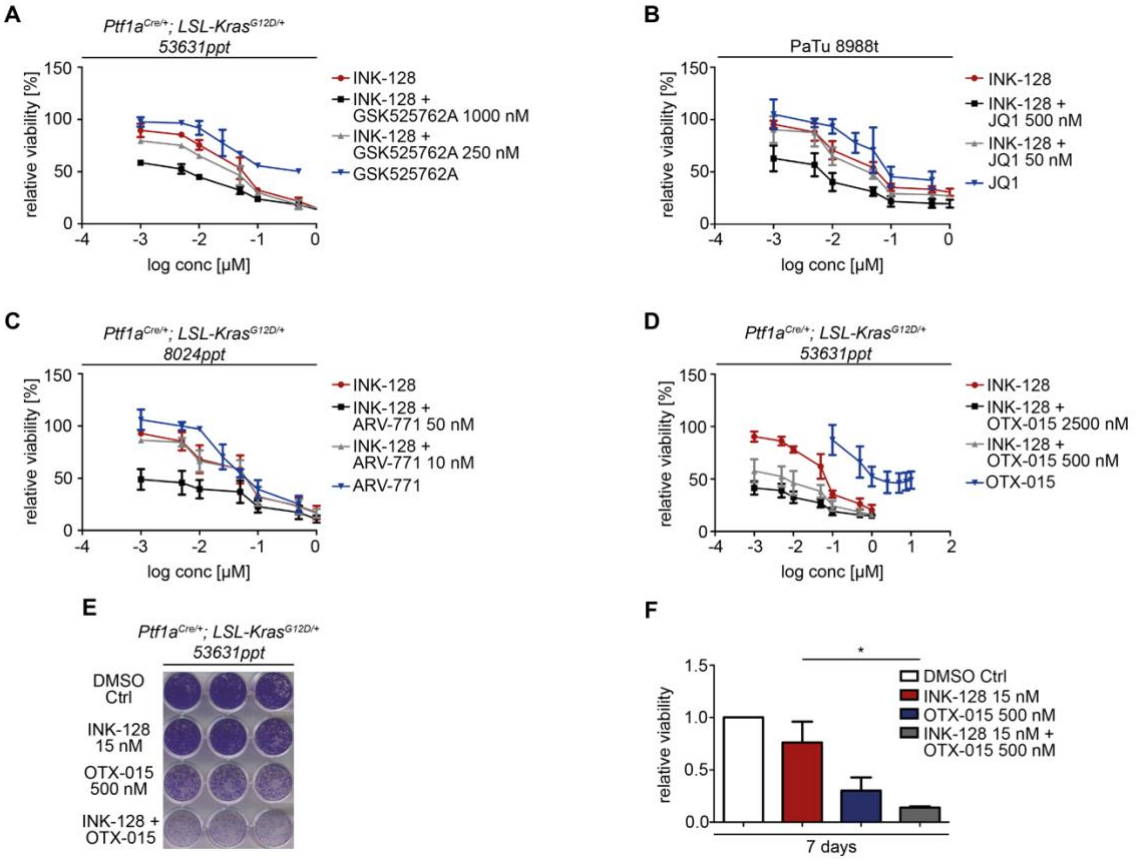

Figure 6. MTOR-based combination therapies with different BET inhibitors.

*(A) – (D) The indicated murine and human cell lines were treated with INK-128, GSK525762A (n=2) / JQ1 (n=3) / ARV-771 (n=3) / OTX-015 (n=4) or in combination therapies. After 72 h the viability was measured in MTT assays. (E) Exemplary clonogenic assay performed as a long-term viability assay with the indicated drug treatment. (F) Quantification of independent biological replicates (n=3) as described in (E). *P-value of a paired Student's t-test =0.0356.*

To systematically quantify the synergism, CI synergy scores based on the Chou-Talalay method were calculated with CompuSyn for all investigated cell lines and BET inhibitors (Figure 7A - D). Combination treatment with OTX-015 showed strong synergistic scores over a wide dose-range and across different murine and human PDAC cell lines (Figure 7B) and was therefore chosen for further experiments.

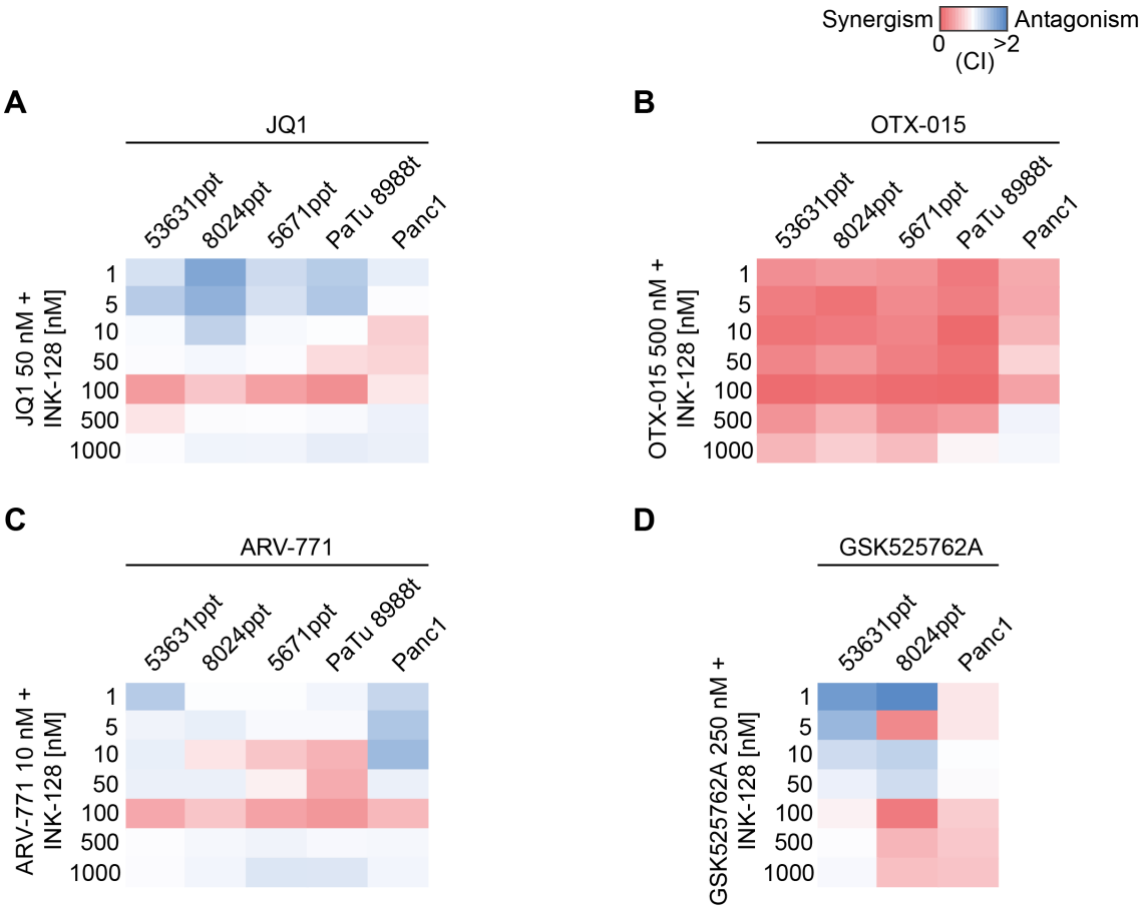

Figure 7. CI-values for combination therapy with INK-128 and various BETi.

(A) – (D) Heatmap with the calculated CI-values for the indicated dual drug treatment (INK-128 + JQ1/OTX-015/ARV-771/GSK525762A) (JQ1: 53631ppt n=3, 8024ppt n=3, 5671ppt n=2, PaTu 8988t n=3, Panc1 n=2; OTX-015: 53631ppt n=4, 8024ppt n=3, 5671ppt n=3, PaTu 8988t n=2, Panc1 n=4; ARV-771: 53631ppt n=4, 8024ppt n=3, 5671ppt n=3, PaTu 8988t n=2, Panc1 n=4; GSK525762A: 53631ppt n=2, 8024ppt n=1, Panc1 n=1).

To extend the study, and test whether the combination works in a large panel of PDAC cell lines, 21 murine *Kras*^{G12D}-driven PDAC cell lines were analyzed in MTT assays with the combination of MTOR (INK-128) and BET (OTX-015) inhibitors. A great degree of heterogeneity was observed in the response to the single treatments with the MTOR or BET inhibitor as demonstrated by the differences in the IC_{50} values (drug concentration with half maximal growth inhibition) (Figure 8A, B). The synergism between the drugs was calculated with the CompuSyn tool based on the Chou-Talalay method (Chou & Talalay, 1984). Even though the response to the single drug treatments was very heterogeneous between the tested PDAC cell lines, almost all screened cell lines showed a high synergism over a wide dose-range (Figure 8C). In addition, the synergism could

be verified by clonogenic assays as well (Figure 8D - G). The cells in the 24-well plate were treated in a 3 x 5 dose combination matrix with INK-128 (25 – 100 nM), OTX-015 (15.36 – 250 nM) or their combination and grown until the DMSO-treated control well was confluent. Two clonogenic assays of the screened PDAC cell lines are shown, the one with the lowest (8248ppt) (Figure 8D) and highest (53631ppt) (Figure 8E) synergy score calculated according to the ZIP method by the SynergyFinder online tool (Figure 8F, G). In the cell line 8248ppt, the growth inhibitory effect due to the MTOR inhibitor alone is already very strong and is not further increased by the BET inhibitor, which is reflected in the isobologramm (Figure 8F) by the low synergism and even slight antagonism as indicated by the negative overall synergy score. In contrast, high synergism across almost the entire dose-combination matrix was observed in the 53631ppt cell line (Figure 8G).

In summary, the synergism between the MTOR and BET inhibitors could be shown across a wide range of PDAC cell lines.

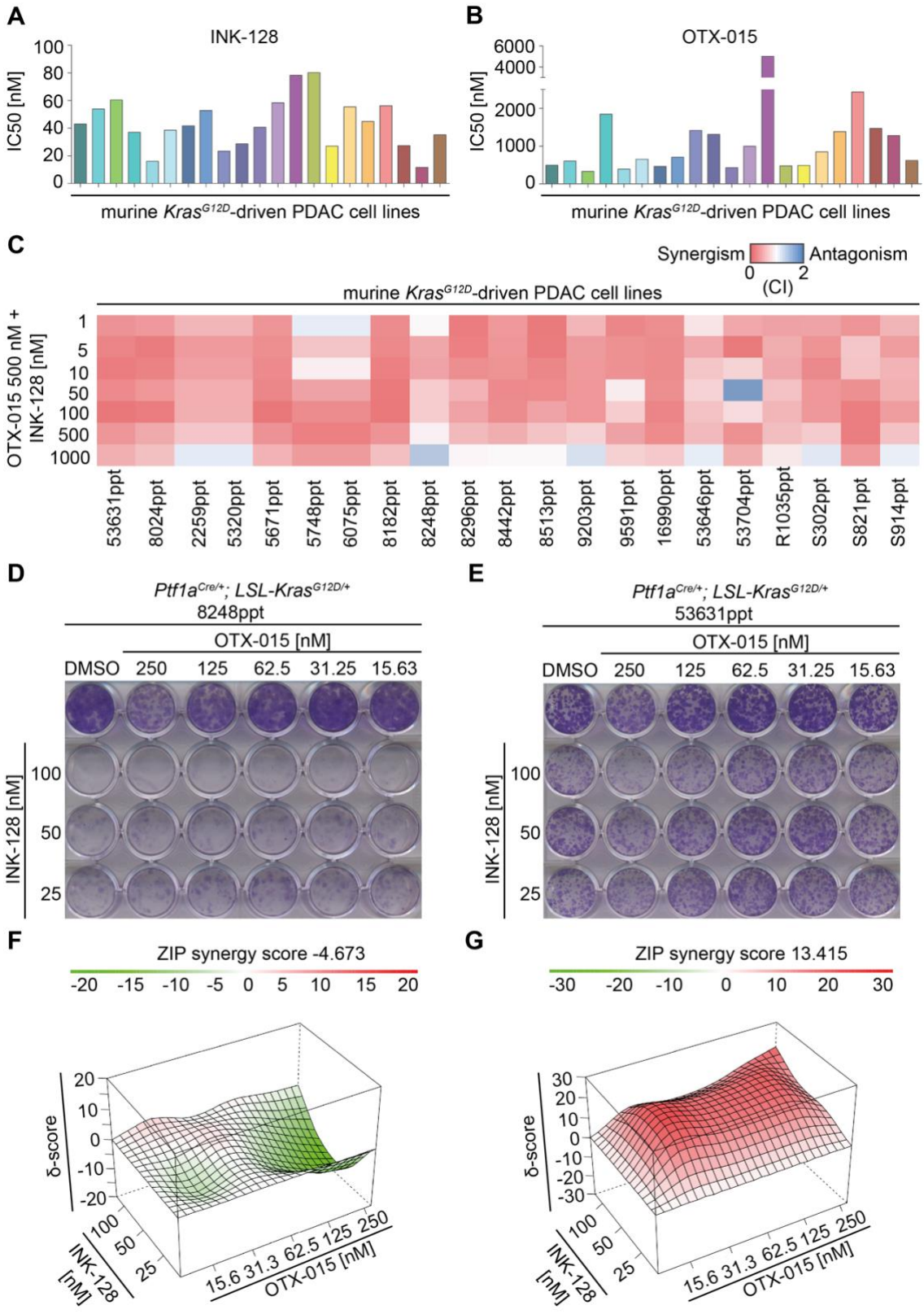

Figure 8. MTOR and BET inhibitors act synergistic.

(A) 21 murine Kras^{G12D}-driven PDAC cell lines treated with INK-128 (1 - 1000 nM) for MTT assay. Large disparities of the cell line specific overall IC_{50} values. (B) Same cell lines as described in (A) treated with OTX-015 (0.02 - 10 µM). For (A) and (B) IC_{50} values determined as a mean of two independent biological replicates (n=2). (C) CI-values for the above

mentioned cell lines after combination treatment with INK-128 (1 - 1000 nM) and OTX-015 (500 nM) (n=2). Combination index calculated with CompuSyn. (D), (E) Long-term clonogenic assays with indicated cell lines and drug treatments showing different sensitivity (n=1). (F), (G) Isobolograms depicting the scans above. 3D representation from SynergyFinder displays the synergistic (red) and antagonistic (green) areas across the entire matrix.

4.5 Mechanism of the synergistic action of the MTOR/BET inhibitor combination

The next aim was to determine, whether the synergistic action of the MTORi and BETi combination was due to the blocking of the above mentioned adaptive rewiring of the ERK and AKT signaling pathways. Although it is already known for other tumor entities that BET inhibitors can block the adaptive rewiring after targeted therapies (Stratikopoulos et al., 2015), this does not seem to be applicable here as both $pAKT^{Thr308}$ and $pERK^{Thr202/Tyr204}$ (Figure 9A, B) (Supplemental Figure 5) were phosphorylated after the combined MTORi and BETi treatment to a similar degree as upon MTOR inhibition alone.

To investigate the cell fate upon combined treatment with INK-128 and OTX-015, cell cycle analysis (Figure 9C) was performed by propidium iodide flow cytometric assay in murine PDAC cells. However, no significant changes in the cell cycle profile compared to the single drug treatments could be observed. While the proteasomal inhibitor Bortezomib strongly induced apoptosis as shown by the increase in the subG1 fraction, the combination of INK-128 + OTX-015 rather induced a G1 arrest but only to a similar degree as upon INK-128 treatment alone.

Next, RNA-Seq with subsequent GSEA was used to identify genes and pathways that might explain the synergistic effects of the MTOR and BET inhibitor combination (Figure 9D).

As expected, MTOR and metabolic signatures were downregulated after INK-128 treatment, while OTX-015 mainly inhibited MYC target genes as demonstrated by the downregulation of MYC signatures, thus confirming the validity of the approach. Cell cycle signatures such as G2M and E2F were initially downregulated upon MTOR inhibition, but upregulated again after 72 hours

together with MYC and oxidative phosphorylation signatures. This indicates that the cells might adapt to the treatment and grow again, when they are only treated with INK-128. After the combination treatment, however, the cell cycle and oxidative phosphorylation but not the MYC signatures, even on protein level (Supplemental Figure 7), remained downregulated even after 72 hours.

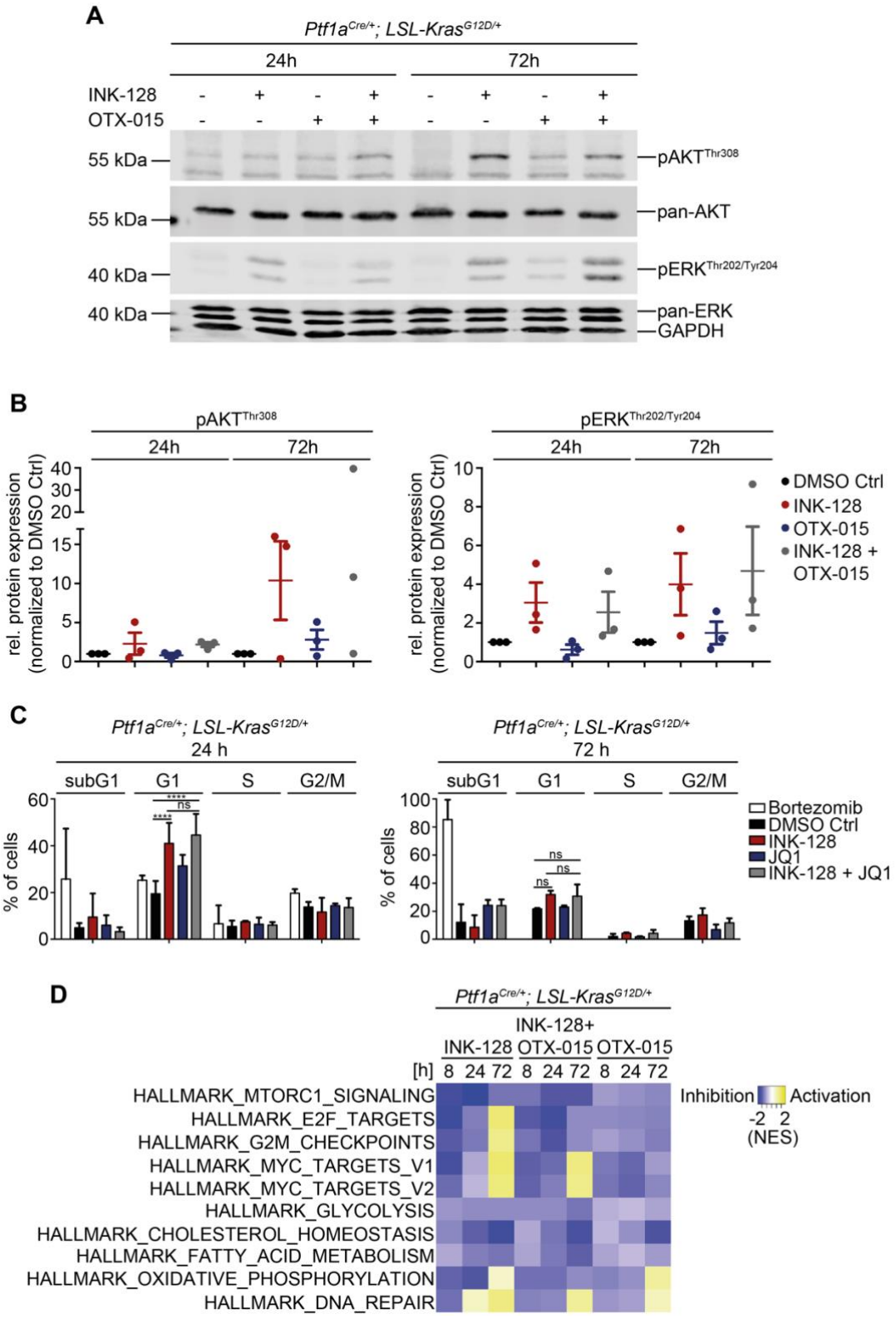

Figure 9. Mechanism of synergistic action of the MTORi and BETi combination.

(A) Ptf1a$^{Cre/+}$; LSL-Kras$^{G12D/+}$ cells were treated with INK-128 (500 nM), OTX-015 (1 µM) and the combination over indicated time. Western blot determines phosphorylation and expression of AKT (Thr308) as well as ERK (Thr202/Tyr204). Same lysates were blotted to different membranes and controlled by pan-AKT or pan-ERK for equal loading. (B) Quantification of independent biological replicates (n=3) as described in (A). The ratio of the

*depicted phospho-protein to pan-protein in DMSO Ctrl was arbitrary set to one. (C) Ptf1a$^{Cre/+}$; LSL-Kras$^{G12D/+}$ cells were treated as indicated for 24 and 72 h. Cells were stained with PI and used for cell cycle analysis. *P-value of an ANOVA test <0.05 (n=3). For (A) and (C) medium with fresh inhibitors was replaced every day. (D) Heat map of the indicated HALLMARK signatures from RNA-Seq data. Ptf1a$^{Cre/+}$; LSL-Kras$^{G12D/+}$ cells treated with INK-128, OTX-015 or their combination for 8, 24 and 72 hours.*

5 Discussion

Previous work from our group demonstrated the adaptive rewiring in the ERK and PI3K signaling pathways after genetic or pharmacological blockage of MTOR in PDAC. The deletion of MTOR lead to an increased phosphorylation of ERK and AKT at the amino acid residues Threonine 308 and Serine 473 in murine PDAC cell lines (Hassan et al., 2018). The lack of therapeutic effects (Rajurkar et al., 2017), as well as tumor progression in mouse models (Driscoll et al., 2016) after treatment with MTOR inhibitors, suggest the establishment of MTOR inhibitor-based combination therapies.

In the first part of the thesis, it was investigated if the adaptive rewiring upon MTOR inhibition occurs via autocrine loops over RTKs and whether this is a targetable vulnerability to overcome the occurring resistance (Nazarian et al., 2010; Prahallad et al., 2012). The RTK Array indeed showed an increased phosphorylation of several RTKs upon MTOR inhibition, out of which AXL might be the most promising finding. Two other promising targets (EGFR and IGFR) were previously tested and pharmacologically inhibited with Gefitinib and Linsitinib in our group. However, no synergism with MTOR inhibition was detected. Therefore, the AXL inhibitor Gilteritinib and two VEGFR inhibitors were investigated in more detail. VEGFR3 was also found to be strongly activated in the RTK array. VEGFR are known to be primarily involved in the lymphangiogenesis but little is known about their role in mediating resistance to targeted therapies (Su et al., 2007). In this study, inhibition of VEGFR with the two VEGFR inhibitors Axitinib and SAR131675 did not further sensitize the cells to MTORi treatment. The third examined inhibitor blocking AXL was Gilteritinib, which was used for the treatment of Fms-like tyrosine kinase 3 mutated relapsed/refractory AML resulting in a clinical benefit of patients and is already approved in Japan and the United States. Moreover, combining Gilteritinib with chemotherapy lead to a reduced tumor volume compared to single agents (Ueno et al., 2019). As known, AXL expression correlates with chemoresistance in various malignancies (Asiedu et al., 2014; Lin et al., 2017). In small-cell lung cancer, it was verified that acquired resistance to WEE1 inhibition could be overcome with an AXL inhibitor (Sen et al., 2017). In head and neck as well as esophageal squamous cell carcinomas the combination treatment with PI3Kα

and AXL inhibitors also overwhelm the resistance to PI3Kα inhibitors (Elkabets et al., 2015). In this study, a synergism of the AXL inhibitor Gliteritinib in combination with the MTOR inhibitor INK-128 was demonstrated in the investigated human PDAC cell line PaTu 8988t, indicating that this might be a promising combination therapy, which warrants further investigation. A more detailed molecular analysis of the possible resistance mechanism to MTOR inhibition driven by AXL activation would be necessary. Furthermore, the combination of MTOR and AXL inhibitor showed a much higher synergism in the human PDAC cell line PaTu 8988t than in the murine PDAC cell line 53631ppt. Therefore, a combinatorial screening in a larger panel of PDAC models should be performed to determine the utility of MTOR and AXL combination therapies and to define PDAC subtypes that are sensitive to the combination.

The calculated CI-values for the AXL inhibitors were wide-ranging and the combination only synergistic in a very narrow dose-range. In this study, just one of the activated RTKs was blocked at a time. However, it may be conceivable that blocking only one of the activated RTKs is not sufficient to overcome the resistance mechanism. For an effective treatment it might therefore be necessary to target multiple of the activated RTKs to block the adaptive rewiring, as has been shown in a study in PDAC, where several RTKs were found to be activated upon MEK inhibition and only combined inhibition of all three co-activated RTKs and MEK was able to inhibit proliferation (Pettazzoni et al., 2015). Another influencing factor is the heterogeneity in the tumor itself, meaning that there are various subclones in the neoplasia, which might activate different signaling pathways in response to targeted therapies (Rambow et al., 2018). In order to address the intratumoral heterogeneity, it would be essential to identify the major subclones via single-cell proteomic approaches and inhibit the different signaling networks that they activate upon targeted therapies (Wei et al., 2016).

In addition to the Phospho-RTK array, RNA-Seq was employed to identify potential pathways involved in the adaptive rewiring. In the murine PDAC cell line PTT-ZH363-*Mtor*$^{\Delta E3/lox}$, an upregulation of NF-κB- and TNFα-signaling was found upon MTOR deletion. In literature, NF-κB has been identified as a key player in cisplatin resistance. The aberrant expression and regulation of NF-κB is involved in the development of various cancer types (Godwin et al., 2013). Besides the impact of NF-κB, TNFα mediates Doxycycline-resistance in primary human

breast cancer and its expression level is correlated with the disease severity (Zhang et al., 2018). IKBKE (inhibitor of nuclear factor kappa-B kinase subunit epsilon), which inhibits the DNA-binding of NF-κB p50-p65 and p50-c-Rel complexes and mediates its activity by a NF-κB-independent mechanism, was found to be required during KRAS-induced pancreatic tumorigenesis. After MTOR blockage, IKBKE promotes the reactivation of AKT, and in line with this, the combined inhibition of IKBKE and MTOR synergistically blocks pancreatic tumor growth together with a significant increase in apoptosis (Rajurkar et al., 2017). Due to this connection and the link between MTOR and NF-κB, three NF-κB inhibitors were investigated for synergistic effects with INK-128 to tackle the adaptive rewiring. In some instances, there was a synergistic effect in a very narrow therapeutic window. However, only a slight change in the dose-response to MTOR inhibition was observed in the PDAC cell lines deficient for RelA compared to their proficient controls, indicating that these factors do not play a significant role in resistance to MTOR inhibition, at least not on their own. The observed upregulation of NF-κB-related gene signatures upon MTOR ablation might be an unspecific stress response rather than a secondary resistance mechanism.

In the second part of the thesis the aim was to identify factors whose perturbation might be synthetically lethal in combination with perturbation of MTOR. The concept of synthetic lethality is defined as one mutation alone out of two genes of a predicted SL pair is compatible with viability but mutation of both leads to apoptosis (Kaelin, 2005). In the context of anticancer therapy, targeting a gene which is synthetic lethal to a cancer-relevant mutation should only kill tumor cells. In PDAC for example, the clinical relevance of this concept is supported by the POLO trial demonstrating that patients with germline BRCA mutations and metastatic pancreatic cancer treated with the PARP inhibitor Olaparib significantly benefit in terms of progression-free survival (Golan et al., 2019). The SynLethDB – a comprehensive database harboring a large set of synthetic lethality pairs – was accessed and out of the top hits, MYC was chosen as the most promising SL pair with MTOR. While MYC is still considered to be undruggable, it can be indirectly targeted by BET inhibitors as transcription of MYC is regulated by BRD4 among others. To test the concept, stable MTOR knockout clones, which were already generated in our group, were treated with BET inhibitors. The MTOR knockout clones were more sensitive towards BET

inhibition than the proficient ones. This indicates that MYC might be an alternative signaling hub to ensure the cellular survival and proliferation upon MTOR deletion. Consequently, the concomitant inhibition of MTOR and MYC might be synergistic and therefore be a therapeutically useful approach.

Among the BET inhibitors tested in a panel of human and murine PDAC cells, OTX-015 showed the highest synergism with the MTORi INK-128. Furthermore, the applicability in the clinic for OTX-015 is promising due to the activity and tolerability in the completed clinical trials (Alqahtani et al., 2019). OTX-015 downregulates MYC and synergism with MTORi and other anticancer agents (Boi et al., 2015; Gaudio et al., 2016) has been shown. Hence, the BET inhibitor OTX-015 was examined more in the following experiments.

The screening of 21 murine $Kras^{G12D}$-driven PDAC cell lines revealed heterogeneity in the response to INK-128 and OTX-015. Therefore, studying the heterogeneity of the tumor itself could be helpful to tackle the occurring secondary resistance of many failed targeted therapies in the clinic. So, for forthcoming stratification of the patients, it is necessary to identify PDAC subtypes or biomarkers which correlate with sensitivity of INK-128. Nonetheless, synergism was demonstrated in many cell lines despite a heterogenous response to single inhibitors at least in the MTT. However, especially in screening the panel of PDAC cell lines with the clonogenic assays only a narrow dose-range (INK-128 25 - 100 nM, OTX-015 15.63 - 250 nM) was investigated that might not be suitable for every cell line and synergy scores might therefore change if investigated in a different dose-range.

Furthermore, the limited efficacy of single agents due to secondary resistance is an unsolved issue of targeted cancer therapies. From literature, it is known that BETi can block adaptive rewiring after targeted therapies in other tumor entities. In a model of metastatic breast cancer driven by PI3K and MYC treated with PI3Ki and BETi, tumor regression and cell death was induced (Stratikopoulos et al., 2015). Moreover, in this setting, BETi blocked the PI3K signaling reactivation after treatment with Pictilisib (GDC-0941), a selective PI3Ki. In lung cancer, YAP1 upregulation was found as a mediator of acquired resistance, which can be defeated with intermittent pulses of JQ1 and furthermore re-sensitize resistant cells to TBK1(TANK-binding kinase 1)/MEK inhibition (Kitajima et al., 2018). In line with these results, in head and neck squamous cell carcinoma, the cetuximab

resistance was repressed with JQ1 (Leonard et al., 2018) and in Ewing sarcoma the IGF1-mediated (insulin-like growth factor 1) autocrine mechanism was suppressed by BET inhibition leading to repressed cell proliferation and survival (Loganathan et al., 2016). In this project, on the contrary, combinatorial treatment with MTORi and BETi in the investigated PDAC cell lines did not block the increased phosphorylation of AKT or ERK upon MTOR inhibition (Hassan et al., 2018), suggesting that the observed synergism in these cell lines is not due to a suppression of the adaptive rewiring of these pathways.

To decipher the mechanism behind the synergism of INK-128 and OTX-015, RNA-Seq was performed. Treating the PDAC cells with INK-128 suppressed the MTOR signaling as expected. The transcription factor MYC was repressed at the early timepoints, but MTOR inhibition alone resulted in an upregulation of MYC at the RNA and protein level after 72 hours. This supports the hypothesis that MYC might ensure cellular survival and resistance to MTOR inhibition. These data are completely consistent with recent work demonstrating that resistance to MTOR inhibition is at least partially mediated through the stabilization of MYC and that decreased MYC expression sensitizes pancreatic cancer cells to MTORi (Allen-Petersen et al., 2019). Although the BETi alone blocked MYC as assumed (Coude et al., 2015; Delmore et al., 2011; Vazquez et al., 2017), as shown by the downregulation of the MYC targets, the combination (MTORi + BETi) treatment was not able to block the upregulation of MYC upon MTOR blockage. However, cell cycle signatures that are strongly connected to MYC signaling such as “HALLMARK_E2F_TARGETS” and “HALLMARK_G2M_CHECKPOINTS” are downregulated after the combination treatment. This could indicate that maybe a subset of MYC-dependent cell cycle genes is dependent on BET signaling and blocked by OTX-015. The strong downregulation of important cell cycle regulators in the combination compared to the single-agent treatment therefore might explain the observed synergistic effects. However, to validate these assumptions further investigations are required.

The PI-flowcytometry analysis showed no increased subG1 population, which marks apoptotic cells. This indicates, that the combination despite the observed synergism is not synthetic lethal. Intriguingly, despite the downregulation of the cell cycle signatures, no significant change in the PI-cell cycle analysis between MTOR and dual blockage was observed. The alteration in the cell cycle profile,

represented by G1 arrest but no increased apoptosis in the examined doses and time points, remained almost the same upon the single agent INK-128 and the combination treatment. However, the PI-cell cycle analysis was only done with one concentration and further dose-ranges should be investigated in the PI-flowcytometry. In addition, more detailed methods such as BrdU (5-bromo-2'-deoxyuridine)-PI-FACS or live cell imaging with cell cycle sensors could help to determine the cell fate upon the combinatorial treatment. Furthermore, investigating the effect of BET inhibition on proficient versus deficient MTOR clones via RNA-Seq and BrdU-PI-FACS might help to elucidate the molecular process relevant for the impaired proliferation.

In addition, the RNA-Seq indicates downregulated OXPHOS (oxidative phosphorylation) signatures in the treatment with MTORi and BETi reflecting the increased metabolic stress. MYC and MTOR are both known to be essential regulators of cellular metabolism. Therefore, one pursuing step might be to examine MYC in the MTOR-deficient clones. On top of that, to determine whether energy metabolism in the cell might be inhibited by the combination treatment, it would be good to perform metabolomics for further insight.

Although the exact molecular mechanisms currently remain unclear, the results suggest options for the establishment of MTORi-based combination therapies. To translate these basic findings to the clinic, a more encompassing understanding of the molecular processes behind the synergism of MTOR and BET inhibition as well as predictive biomarkers for this combination are needed.

6 Conclusion

The aims of the present thesis were to decipher and target the molecular mechanism behind the adaptive rewiring in ERK and PI3K signaling pathways upon MTOR inhibition in pancreatic cancer and secondly identify factors whose perturbation might be synergistic with MTORi. For investigating MTORi-based combination therapies for PDAC, which is largely resistant to current standard therapies, several targets were investigated in established murine and human PDAC cell lines. The idea to block the rising resistance via inhibiting upregulated RTKs after MTOR inhibition like AXL showed slight synergism indicating that this might be a combination to study further. Targeting the upregulation of NF-κB upon MTOR deletion with IKK inhibitors did not result in strong synergistic effects. A search of SL pairs in the synthetic lethality database SynLethDB indicated that MTOR and MYC might be together synthetically lethal. MYC, still considered to be undruggable, was indirectly targeted with BETi. MTOR deficient clones were more sensitive towards BET inhibition and combined MTOR and BET inhibition revealed a synergistic effect. Cell cycle genes were downregulated in the combination, indicating that this might explain the observed synergistic effects, but further research on the exact cell fate upon the combination treatment will be necessary as there was no apoptosis or significant change demonstrated in the cell cycle analysis within the examined period.

In order to translate these findings into the clinic, it will be necessary to identify responsive subgroups of PDAC as well as predictive biomarkers for these combinatorial treatments. Further, more detailed preclinical and clinical research into the synergism of MYC and MTOR and the role of BET proteins is needed to gain an improved understanding of this concept.

List of figures

List of tables

References

Afgan, E., Baker, D., van den Beek, M., Blankenberg, D., Bouvier, D., Cech, M., Chilton, J., Clements, D., Coraor, N., Eberhard, C., Gruning, B., Guerler, A., Hillman-Jackson, J., Von Kuster, G., Rasche, E., Soranzo, N., Turaga, N., Taylor, J., Nekrutenko, A., & Goecks, J. (2016, Jul 8). The Galaxy platform for accessible, reproducible and collaborative biomedical analyses: 2016 update. *Nucleic Acids Res, 44*(W1), W3-w10. https://doi.org/10.1093/nar/gkw343

Agarwal, A., & Saif, M. W. (2014, Jul 28). KRAS in pancreatic cancer. *Jop, 15*(4), 303-305. https://doi.org/10.6092/1590-8577/2660

Allen-Petersen, B. L., Risom, T., Feng, Z., Wang, Z., Jenny, Z. P., Thoma, M. C., Pelz, K. R., Morton, J. P., Sansom, O. J., Lopez, C. D., Sheppard, B., Christensen, D. J., Ohlmeyer, M., Narla, G., & Sears, R. C. (2019, Jan 1). Activation of PP2A and Inhibition of mTOR Synergistically Reduce MYC Signaling and Decrease Tumor Growth in Pancreatic Ductal Adenocarcinoma. *Cancer Res, 79*(1), 209-219. https://doi.org/10.1158/0008-5472.Can-18-0717

Alqahtani, A., Choucair, K., Ashraf, M., Hammouda, D. M., Alloghbi, A., Khan, T., Senzer, N., & Nemunaitis, J. (2019, Mar). Bromodomain and extra-terminal motif inhibitors: a review of preclinical and clinical advances in cancer therapy. *Future Sci OA, 5*(3), Fso372. https://doi.org/10.4155/fsoa-2018-0115

Asiedu, M. K., Beauchamp-Perez, F. D., Ingle, J. N., Behrens, M. D., Radisky, D. C., & Knutson, K. L. (2014, Mar 6). AXL induces epithelial-to-mesenchymal transition and regulates the function of breast cancer stem cells. *Oncogene, 33*(10), 1316-1324. https://doi.org/10.1038/onc.2013.57

Bennett, R. L., & Licht, J. D. (2018, Jan 6). Targeting Epigenetics in Cancer. *Annu Rev Pharmacol Toxicol, 58*, 187-207. https://doi.org/10.1146/annurev-pharmtox-010716-105106

Boi, M., Gaudio, E., Bonetti, P., Kwee, I., Bernasconi, E., Tarantelli, C., Rinaldi, A., Testoni, M., Cascione, L., Ponzoni, M., Mensah, A. A., Stathis, A., Stussi, G., Riveiro, M. E., Herait, P., Inghirami, G., Cvitkovic, E., Zucca, E., & Bertoni, F. (2015, Apr 1). The BET Bromodomain Inhibitor OTX015 Affects Pathogenetic Pathways in Preclinical B-cell Tumor Models and Synergizes with Targeted Drugs. *Clin Cancer Res, 21*(7), 1628-1638. https://doi.org/10.1158/1078-0432.Ccr-14-1561

Bosetti, C., Lucenteforte, E., Silverman, D. T., Petersen, G., Bracci, P. M., Ji, B. T., Negri, E., Li, D., Risch, H. A., Olson, S. H., Gallinger, S., Miller, A. B., Bueno-de-Mesquita, H. B., Talamini, R., Polesel, J., Ghadirian, P., Baghurst, P. A., Zatonski, W., Fontham, E., Bamlet, W. R., Holly, E. A., Bertuccio, P., Gao, Y. T., Hassan, M., Yu, H., Kurtz, R. C., Cotterchio, M., Su, J., Maisonneuve, P., Duell, E. J., Boffetta, P., & La Vecchia, C. (2012, Jul). Cigarette smoking and pancreatic cancer: an analysis from the International Pancreatic Cancer Case-Control Consortium (Panc4). *Ann Oncol, 23*(7), 1880-1888. https://doi.org/10.1093/annonc/mdr541

Bradford, M. M. (1976, May 7). A rapid and sensitive method for the quantitation of microgram quantities of protein utilizing the principle of protein-dye binding. *Anal Biochem, 72*, 248-254. https://www.sciencedirect.com/science/article/pii/0003269776905273?via%3Dihub

Braeuer, S. J., Büneker, C., Mohr, A., & Zwacka, R. M. (2006). Constitutively Activated Nuclear Factor-κB, but not Induced NF-κB, Leads to TRAIL Resistance by Up-Regulation of X-Linked Inhibitor of Apoptosis Protein in Human Cancer Cells. *Molecular Cancer Research, 4*(10), 715-728. https://doi.org/10.1158/1541-7786.Mcr-05-0231

Castellano, E., & Downward, J. (2011, Mar). RAS Interaction with PI3K: More Than Just Another Effector Pathway. *Genes Cancer, 2*(3), 261-274. https://doi.org/10.1177/1947601911408079

Chaturvedi, M., Sung, B., Yadav, V., Kannappan, R., & Aggarwal, B. (2011, Apr 7). NF-κB addiction and its role in cancer: 'one size does not fit all'. *Oncogene, 30*(14), 1615-1630. https://doi.org/10.1038/onc.2010.566

Cheng, Z., Gong, Y., Ma, Y., Lu, K., Lu, X., Pierce, L. A., Thompson, R. C., Muller, S., Knapp, S., & Wang, J. (2013, Apr 1). Inhibition of BET bromodomain targets genetically diverse glioblastoma. *Clin Cancer Res, 19*(7), 1748-1759. https://doi.org/10.1158/1078-0432.Ccr-12-3066

Chou, T. C., & Talalay, P. (1984). Quantitative analysis of dose-effect relationships: the combined effects of multiple drugs or enzyme inhibitors. *Adv Enzyme Regul, 22*, 27-55.

Conradt, L., Henrich, A., Wirth, M., Reichert, M., Lesina, M., Algül, H., Schmid, R. M., Krämer, O. H., Saur, D., & Schneider, G. (2013, May 15). Mdm2 inhibitors synergize with topoisomerase II inhibitors to induce p53-independent pancreatic cancer cell death. *Int J Cancer, 132*(10), 2248-2257. https://doi.org/10.1002/ijc.27916

Coude, M. M., Braun, T., Berrou, J., Dupont, M., Bertrand, S., Masse, A., Raffoux, E., Itzykson, R., Delord, M., Riveiro, M. E., Herait, P., Baruchel, A., Dombret, H., & Gardin, C. (2015, Jul 10). BET inhibitor OTX015 targets BRD2 and BRD4 and decreases c-MYC in acute leukemia cells. *Oncotarget, 6*(19), 17698-17712. https://doi.org/10.18632/oncotarget.4131

Delmore, J. E., Issa, G. C., Lemieux, M. E., Rahl, P. B., Shi, J., Jacobs, H. M., Kastritis, E., Gilpatrick, T., Paranal, R. M., Qi, J., Chesi, M., Schinzel, A. C., McKeown, M. R., Heffernan, T. P., Vakoc, C. R., Bergsagel, P. L., Ghobrial, I. M., Richardson, P. G., Young, R. A., Hahn, W. C., Anderson, K. C., Kung, A. L., Bradner, J. E., & Mitsiades, C. S. (2011, Sep 16). BET bromodomain inhibition as a therapeutic strategy to target c-Myc. *Cell, 146*(6), 904-917. https://doi.org/10.1016/j.cell.2011.08.017

Doroshow, D. B., Eder, J. P., & LoRusso, P. M. (2017). BET inhibitors: a novel epigenetic approach. *Annals of Oncology, 28*(8), 1776-1787. https://doi.org/10.1093/annonc/mdx157

Driscoll, D. R., Karim, S. A., Sano, M., Gay, D. M., Jacob, W., Yu, J., Mizukami, Y., Gopinathan, A., Jodrell, D. I., Evans, T. R., Bardeesy, N., Hall, M. N., Quattrochi, B. J., Klimstra, D. S., Barry, S. T., Sansom, O. J., Lewis, B. C., & Morton, J. P. (2016, Dec 1). mTORC2 Signaling Drives the Development

and Progression of Pancreatic Cancer. *Cancer Res, 76*(23), 6911-6923. https://doi.org/10.1158/0008-5472.Can-16-0810

Elkabets, M., Pazarentzos, E., Juric, D., Sheng, Q., Pelossof, R. A., Brook, S., Benzaken, A. O., Rodon, J., Morse, N., Yan, J. J., Liu, M., Das, R., Chen, Y., Tam, A., Wang, H., Liang, J., Gurski, J. M., Kerr, D. A., Rosell, R., Teixido, C., Huang, A., Ghossein, R. A., Rosen, N., Bivona, T. G., Scaltriti, M., & Baselga, J. (2015, Apr 13). AXL mediates resistance to PI3Kalpha inhibition by activating the EGFR/PKC/mTOR axis in head and neck and esophageal squamous cell carcinomas. *Cancer Cell, 27*(4), 533-546. https://doi.org/10.1016/j.ccell.2015.03.010

Eser, S., Reiff, N., Messer, M., Seidler, B., Gottschalk, K., Dobler, M., Hieber, M., Arbeiter, A., Klein, S., Kong, B., Michalski, C. W., Schlitter, A. M., Esposito, I., Kind, A. J., Rad, L., Schnieke, A. E., Baccarini, M., Alessi, D. R., Rad, R., Schmid, R. M., Schneider, G., & Saur, D. (2013, Mar 18). Selective requirement of PI3K/PDK1 signaling for Kras oncogene-driven pancreatic cell plasticity and cancer. *Cancer Cell, 23*(3), 406-420. https://doi.org/10.1016/j.ccr.2013.01.023

Faller, W. J., Jackson, T. J., Knight, J. R., Ridgway, R. A., Jamieson, T., Karim, S. A., Jones, C., Radulescu, S., Huels, D. J., Myant, K. B., Dudek, K. M., Casey, H. A., Scopelliti, A., Cordero, J. B., Vidal, M., Pende, M., Ryazanov, A. G., Sonenberg, N., Meyuhas, O., Hall, M. N., Bushell, M., Willis, A. E., & Sansom, O. J. (2015, Jan 22). mTORC1-mediated translational elongation limits intestinal tumour initiation and growth. *Nature, 517*(7535), 497-500. https://doi.org/10.1038/nature13896

Filippakopoulos, P., Qi, J., Picaud, S., Shen, Y., Smith, W. B., Fedorov, O., Morse, E. M., Keates, T., Hickman, T. T., Felletar, I., Philpott, M., Munro, S., McKeown, M. R., Wang, Y., Christie, A. L., West, N., Cameron, M. J., Schwartz, B., Heightman, T. D., La Thangue, N., French, C. A., Wiest, O., Kung, A. L., Knapp, S., & Bradner, J. E. (2010, Dec 23). Selective inhibition of BET bromodomains. *Nature, 468*(7327), 1067-1073. https://doi.org/10.1038/nature09504

Frias, M. A., Thoreen, C. C., Jaffe, J. D., Schroder, W., Sculley, T., Carr, S. A., & Sabatini, D. M. (2006, Sep 19). mSin1 is necessary for Akt/PKB phosphorylation, and its isoforms define three distinct mTORC2s. *Curr Biol, 16*(18), 1865-1870. https://doi.org/10.1016/j.cub.2006.08.001

Garcia, P. L., Miller, A. L., Kreitzburg, K. M., Council, L. N., Gamblin, T. L., Christein, J. D., Heslin, M. J., Arnoletti, J. P., Richardson, J. H., Chen, D., Hanna, C. A., Cramer, S. L., Yang, E. S., Qi, J., Bradner, J. E., & Yoon, K. J. (2016, Feb 18). The BET bromodomain inhibitor JQ1 suppresses growth of pancreatic ductal adenocarcinoma in patient-derived xenograft models. *Oncogene, 35*(7), 833-845. https://doi.org/10.1038/onc.2015.126

Garrido-Laguna, I., Tan, A. C., Uson, M., Angenendt, M., Ma, W. W., Villaroel, M. C., Zhao, M., Rajeshkumar, N. V., Jimeno, A., Donehower, R., Iacobuzio-Donahue, C., Barrett, M., Rudek, M. A., Rubio-Viqueira, B., Laheru, D., & Hidalgo, M. (2010, Aug 24). Integrated preclinical and clinical development of mTOR inhibitors in pancreatic cancer. *Br J Cancer, 103*(5), 649-655. https://doi.org/10.1038/sj.bjc.6605819

Gaudio, E., Tarantelli, C., Ponzoni, M., Odore, E., Rezai, K., Bernasconi, E., Cascione, L., Rinaldi, A., Stathis, A., Riveiro, E., Cvitkovic, E., Zucca, E.,

& Bertoni, F. (2016, Sep 6). Bromodomain inhibitor OTX015 (MK-8628) combined with targeted agents shows strong in vivo antitumor activity in lymphoma. *Oncotarget, 7*(36), 58142-58147. https://doi.org/10.18632/oncotarget.10983

Godwin, P., Baird, A. M., Heavey, S., Barr, M. P., O'Byrne, K. J., & Gately, K. (2013). Targeting nuclear factor-kappa B to overcome resistance to chemotherapy. *Front Oncol, 3*, 120. https://doi.org/10.3389/fonc.2013.00120

Goecks, J., Eberhard, C., Too, T., Nekrutenko, A., & Taylor, J. (2013, Jun 13). Web-based visual analysis for high-throughput genomics. *BMC Genomics, 14*, 397. https://doi.org/10.1186/1471-2164-14-397

Golan, T., Hammel, P., Reni, M., Van Cutsem, E., Macarulla, T., Hall, M. J., Park, J. O., Hochhauser, D., Arnold, D., Oh, D. Y., Reinacher-Schick, A., Tortora, G., Algul, H., O'Reilly, E. M., McGuinness, D., Cui, K. Y., Schlienger, K., Locker, G. Y., & Kindler, H. L. (2019, Jul 25). Maintenance Olaparib for Germline BRCA-Mutated Metastatic Pancreatic Cancer. *N Engl J Med, 381*(4), 317-327. https://doi.org/10.1056/NEJMoa1903387

Grandage, V. L., Gale, R. E., Linch, D. C., & Khwaja, A. (2005, Apr). PI3-kinase/Akt is constitutively active in primary acute myeloid leukaemia cells and regulates survival and chemoresistance via NF-kappaB, Mapkinase and p53 pathways. *Leukemia, 19*(4), 586-594. https://doi.org/10.1038/sj.leu.2403653

Guerra, C., Schuhmacher, A. J., Canamero, M., Grippo, P. J., Verdaguer, L., Perez-Gallego, L., Dubus, P., Sandgren, E. P., & Barbacid, M. (2007, Mar). Chronic pancreatitis is essential for induction of pancreatic ductal adenocarcinoma by K-Ras oncogenes in adult mice. *Cancer Cell, 11*(3), 291-302. https://doi.org/10.1016/j.ccr.2007.01.012

Guo, J., Liu, H., & Zheng, J. (2016, Jan 4). SynLethDB: synthetic lethality database toward discovery of selective and sensitive anticancer drug targets. *Nucleic Acids Res, 44*(D1), D1011-1017. https://doi.org/10.1093/nar/gkv1108

Hassan, B., Akcakanat, A., Sangai, T., Evans, K. W., Adkins, F., Eterovic, A. K., Zhao, H., Chen, K., Chen, H., Do, K. A., Xie, S. M., Holder, A. M., Naing, A., Mills, G. B., & Meric-Bernstam, F. (2014, Sep). Catalytic mTOR inhibitors can overcome intrinsic and acquired resistance to allosteric mTOR inhibitors. *Oncotarget, 5*(18), 8544-8557. https://www.ncbi.nlm.nih.gov/pmc/articles/PMC4226703/pdf/oncotarget-05-8544.pdf

Hassan, Z., Schneeweis, C., Wirth, M., Veltkamp, C., Dantes, Z., Feuerecker, B., Ceyhan, G. O., Knauer, S. K., Weichert, W., Schmid, R. M., Stauber, R., Arlt, A., Kramer, O. H., Rad, R., Reichert, M., Saur, D., & Schneider, G. (2018, Feb 6). MTOR inhibitor-based combination therapies for pancreatic cancer. *Br J Cancer, 118*(3), 366-377. https://doi.org/10.1038/bjc.2017.421

Hessmann, E., Schneider, G., Ellenrieder, V., & Siveke, J. T. (2016, Mar 31). MYC in pancreatic cancer: novel mechanistic insights and their translation into therapeutic strategies. *Oncogene, 35*(13), 1609-1618. https://doi.org/10.1038/onc.2015.216

Hingorani, S. R., Petricoin, E. F., Maitra, A., Rajapakse, V., King, C., Jacobetz, M. A., Ross, S., Conrads, T. P., Veenstra, T. D., Hitt, B. A., Kawaguchi, Y., Johann, D., Liotta, L. A., Crawford, H. C., Putt, M. E., Jacks, T., Wright, C. V., Hruban, R. H., Lowy, A. M., & Tuveson, D. A. (2003, Dec). Preinvasive and invasive ductal pancreatic cancer and its early detection in the mouse. *Cancer Cell, 4*(6), 437-450. https://www.cell.com/cancer-cell/pdf/S1535-6108(03)00309-X.pdf

Hoesel, B., & Schmid, J. A. (2013). The complexity of NF-κB signaling in inflammation and cancer. *Mol Cancer, 12*, 86. https://doi.org/10.1186/1476-4598-12-86

Ianevski, A., He, L., Aittokallio, T., & Tang, J. (2017, Aug 1). SynergyFinder: a web application for analyzing drug combination dose-response matrix data. *Bioinformatics, 33*(15), 2413-2415. https://doi.org/10.1093/bioinformatics/btx162

Inoki, K., Li, Y., Xu, T., & Guan, K. L. (2003, Aug 1). Rheb GTPase is a direct target of TSC2 GAP activity and regulates mTOR signaling. *Genes Dev, 17*(15), 1829-1834. https://doi.org/10.1101/gad.1110003

Iriana, S., Ahmed, S., Gong, J., Annamalai, A. A., Tuli, R., & Hendifar, A. E. (2016). Targeting mTOR in Pancreatic Ductal Adenocarcinoma. *Front Oncol, 6*, 99. https://doi.org/10.3389/fonc.2016.00099

Janku, F., Yap, T. A., & Meric-Bernstam, F. (2018, Mar 6). Targeting the PI3K pathway in cancer: are we making headway? *Nat Rev Clin Oncol*. https://doi.org/10.1038/nrclinonc.2018.28

Kaelin, W. G. (2005, 2005/09/01). The Concept of Synthetic Lethality in the Context of Anticancer Therapy. *Nature Reviews Cancer, 5*(9), 689-698. https://doi.org/10.1038/nrc1691

Kaizuka, T., Hara, T., Oshiro, N., Kikkawa, U., Yonezawa, K., Takehana, K., Iemura, S., Natsume, T., & Mizushima, N. (2010, Jun 25). Tti1 and Tel2 are critical factors in mammalian target of rapamycin complex assembly. *J Biol Chem, 285*(26), 20109-20116. https://doi.org/10.1074/jbc.M110.121699

Kitajima, S., Asahina, H., Chen, T., Guo, S., Quiceno, L. G., Cavanaugh, J. D., Merlino, A. A., Tange, S., Terai, H., Kim, J. W., Wang, X., Zhou, S., Xu, M., Wang, S., Zhu, Z., Thai, T. C., Takahashi, C., Wang, Y., Neve, R., Stinson, S., Tamayo, P., Watanabe, H., Kirschmeier, P. T., Wong, K. K., & Barbie, D. A. (2018, Sep 10). Overcoming Resistance to Dual Innate Immune and MEK Inhibition Downstream of KRAS. *Cancer Cell, 34*(3), 439-452.e436. https://doi.org/10.1016/j.ccell.2018.08.009

Kleeff, J., Korc, M., Apte, M., La Vecchia, C., Johnson, C. D., Biankin, A. V., Neale, R. E., Tempero, M., Tuveson, D. A., Hruban, R. H., & Neoptolemos, J. P. (2016, Apr 21). Pancreatic cancer. *Nat Rev Dis Primers, 2*, 16022. https://doi.org/10.1038/nrdp.2016.22

Knudsen, E. S., O'Reilly, E. M., Brody, J. R., & Witkiewicz, A. K. (2016, Jan). Genetic Diversity of Pancreatic Ductal Adenocarcinoma and Opportunities for Precision Medicine. *Gastroenterology, 150*(1), 48-63. https://doi.org/10.1053/j.gastro.2015.08.056

Kong, B., Wu, W., Cheng, T., Schlitter, A. M., Qian, C., Bruns, P., Jian, Z., Jager, C., Regel, I., Raulefs, S., Behler, N., Irmler, M., Beckers, J., Friess, H.,

Erkan, M., Siveke, J. T., Tannapfel, A., Hahn, S. A., Theis, F. J., Esposito, I., Kleeff, J., & Michalski, C. W. (2016, Apr). A subset of metastatic pancreatic ductal adenocarcinomas depends quantitatively on oncogenic Kras/Mek/Erk-induced hyperactive mTOR signalling. *Gut, 65*(4), 647-657. https://doi.org/10.1136/gutjnl-2014-307616

Kurimchak, A. M., Shelton, C., Herrera-Montávez, C., Duncan, K. E., Chernoff, J., & Duncan, J. S. (2019, Aug). Intrinsic Resistance to MEK Inhibition through BET Protein-Mediated Kinome Reprogramming in NF1-Deficient Ovarian Cancer. *Mol Cancer Res, 17*(8), 1721-1734. https://doi.org/10.1158/1541-7786.Mcr-18-1332

Laplante, M., & Sabatini, D. M. (2012, Apr 13). mTOR signaling in growth control and disease. *Cell, 149*(2), 274-293. https://doi.org/10.1016/j.cell.2012.03.017

Leonard, B., Brand, T. M., O'Keefe, R. A., Lee, E. D., Zeng, Y., Kemmer, J. D., Li, H., Grandis, J. R., & Bhola, N. E. (2018, Aug 1). BET Inhibition Overcomes Receptor Tyrosine Kinase-Mediated Cetuximab Resistance in HNSCC. *Cancer Res, 78*(15), 4331-4343. https://doi.org/10.1158/0008-5472.Can-18-0459

Lin, J. Z., Wang, Z. J., De, W., Zheng, M., Xu, W. Z., Wu, H. F., Armstrong, A., & Zhu, J. G. (2017, Jun 20). Targeting AXL overcomes resistance to docetaxel therapy in advanced prostate cancer. *Oncotarget, 8*(25), 41064-41077. https://doi.org/10.18632/oncotarget.17026

Lockwood, W. W., Zejnullahu, K., Bradner, J. E., & Varmus, H. (2012, Nov 20). Sensitivity of human lung adenocarcinoma cell lines to targeted inhibition of BET epigenetic signaling proteins. *Proc Natl Acad Sci U S A, 109*(47), 19408-19413. https://doi.org/10.1073/pnas.1216363109

Loganathan, S. N., Tang, N., Fleming, J. T., Ma, Y., Guo, Y., Borinstein, S. C., Chiang, C., & Wang, J. (2016, Jul 12). BET bromodomain inhibitors suppress EWS-FLI1-dependent transcription and the IGF1 autocrine mechanism in Ewing sarcoma. *Oncotarget, 7*(28), 43504-43517. https://doi.org/10.18632/oncotarget.9762

Macosko, E. Z., Basu, A., Satija, R., Nemesh, J., Shekhar, K., Goldman, M., Tirosh, I., Bialas, A. R., Kamitaki, N., Martersteck, E. M., Trombetta, J. J., Weitz, D. A., Sanes, J. R., Shalek, A. K., Regev, A., & McCarroll, S. A. (2015, May 21). Highly Parallel Genome-wide Expression Profiling of Individual Cells Using Nanoliter Droplets. *Cell, 161*(5), 1202-1214. https://doi.org/10.1016/j.cell.2015.05.002

Mazur, P. K., Herner, A., Mello, S. S., Wirth, M., Hausmann, S., Sanchez-Rivera, F. J., Lofgren, S. M., Kuschma, T., Hahn, S. A., Vangala, D., Trajkovic-Arsic, M., Gupta, A., Heid, I., Noel, P. B., Braren, R., Erkan, M., Kleeff, J., Sipos, B., Sayles, L. C., Heikenwalder, M., Hessmann, E., Ellenrieder, V., Esposito, I., Jacks, T., Bradner, J. E., Khatri, P., Sweet-Cordero, E. A., Attardi, L. D., Schmid, R. M., Schneider, G., Sage, J., & Siveke, J. T. (2015, Oct). Combined inhibition of BET family proteins and histone deacetylases as a potential epigenetics-based therapy for pancreatic ductal adenocarcinoma. *Nat Med, 21*(10), 1163-1171. https://doi.org/10.1038/nm.3952

McCleland, M. L., Mesh, K., Lorenzana, E., Chopra, V. S., Segal, E., Watanabe, C., Haley, B., Mayba, O., Yaylaoglu, M., Gnad, F., & Firestein, R. (2016, Feb). CCAT1 is an enhancer-templated RNA that predicts BET sensitivity in colorectal cancer. *J Clin Invest, 126*(2), 639-652. https://doi.org/10.1172/jci83265

Melo, D., Porto, A., Cheverud, J. M., & Marroig, G. (2016). Modularity: Genes, Development, and Evolution. *Annual Review of Ecology, Evolution, and Systematics, 47*(1), 463-486. https://doi.org/10.1146/annurev-ecolsys-121415-032409

Mertz, J. A., Conery, A. R., Bryant, B. M., Sandy, P., Balasubramanian, S., Mele, D. A., Bergeron, L., & Sims, R. J. (2011, Oct 4). Targeting MYC dependence in cancer by inhibiting BET bromodomains. *Proc Natl Acad Sci U S A, 108*(40), 16669-16674. https://doi.org/10.1073/pnas.1108190108

Morran, D. C., Wu, J., Jamieson, N. B., Mrowinska, A., Kalna, G., Karim, S. A., Au, A. Y., Scarlett, C. J., Chang, D. K., Pajak, M. Z., Oien, K. A., McKay, C. J., Carter, C. R., Gillen, G., Champion, S., Pimlott, S. L., Anderson, K. I., Evans, T. R., Grimmond, S. M., Biankin, A. V., Sansom, O. J., & Morton, J. P. (2014, Sep). Targeting mTOR dependency in pancreatic cancer. *Gut, 63*(9), 1481-1489. https://doi.org/10.1136/gutjnl-2013-306202

Mosmann, T. (1983, Dec 16). Rapid colorimetric assay for cellular growth and survival: application to proliferation and cytotoxicity assays. *J Immunol Methods, 65*(1-2), 55-63. https://www.sciencedirect.com/science/article/pii/0022175983903034?via%3Dihub

Murthy, D., Attri, K. S., & Singh, P. K. (2018). Phosphoinositide 3-Kinase Signaling Pathway in Pancreatic Ductal Adenocarcinoma Progression, Pathogenesis, and Therapeutics. *Front Physiol, 9*, 335. https://doi.org/10.3389/fphys.2018.00335

Nakanishi, C., & Toi, M. (2005, Apr). Nuclear factor-kappaB inhibitors as sensitizers to anticancer drugs. *Nat Rev Cancer, 5*(4), 297-309. https://doi.org/10.1038/nrc1588

Nazarian, R., Shi, H., Wang, Q., Kong, X., Koya, R. C., Lee, H., Chen, Z., Lee, M. K., Attar, N., Sazegar, H., Chodon, T., Nelson, S. F., McArthur, G., Sosman, J. A., Ribas, A., & Lo, R. S. (2010, Dec 16). Melanomas acquire resistance to B-RAF(V600E) inhibition by RTK or N-RAS upregulation. *Nature, 468*(7326), 973-977. https://doi.org/10.1038/nature09626

Ossewaarde, J. M., de Vries, A., Bestebroer, T., & Angulo, A. F. (1996, Feb). Application of a Mycoplasma group-specific PCR for monitoring decontamination of Mycoplasma-infected Chlamydia sp. strains. *Appl Environ Microbiol, 62*(2), 328-331. https://doi.org/10.1128/aem.62.2.328-331.1996

Parekh, S., Ziegenhain, C., Vieth, B., Enard, W., & Hellmann, I. (2016, May 9). The impact of amplification on differential expression analyses by RNA-seq. *Sci Rep, 6*, 25533. https://doi.org/10.1038/srep25533

Parkin, D. M. (2011, Dec 6). 2. Tobacco-attributable cancer burden in the UK in 2010. *Br J Cancer, 105 Suppl 2*, S6-s13. https://doi.org/10.1038/bjc.2011.475

Pearce, L. R., Sommer, E. M., Sakamoto, K., Wullschleger, S., & Alessi, D. R. (2011, May 15). Protor-1 is required for efficient mTORC2-mediated activation of SGK1 in the kidney. *Biochem J, 436*(1), 169-179. https://doi.org/10.1042/bj20102103

Pérez-Salvia, M., & Esteller, M. (2017). Bromodomain inhibitors and cancer therapy: From structures to applications. *Epigenetics, 12*(5), 323-339. https://doi.org/10.1080/15592294.2016.1265710

Peterson, T. R., Laplante, M., Thoreen, C. C., Sancak, Y., Kang, S. A., Kuehl, W. M., Gray, N. S., & Sabatini, D. M. (2009, May 29). DEPTOR is an mTOR inhibitor frequently overexpressed in multiple myeloma cells and required for their survival. *Cell, 137*(5), 873-886. https://doi.org/10.1016/j.cell.2009.03.046

Pettazzoni, P., Viale, A., Shah, P., Carugo, A., Ying, H., Wang, H., Genovese, G., Seth, S., Minelli, R., Green, T., Huang-Hobbs, E., Corti, D., Sanchez, N., Nezi, L., Marchesini, M., Kapoor, A., Yao, W., Francesco, M. E., Petrocchi, A., Deem, A. K., Scott, K., Colla, S., Mills, G. B., Fleming, J. B., Heffernan, T. P., Jones, P., Toniatti, C., DePinho, R. A., & Draetta, G. F. (2015, Mar 15). Genetic events that limit the efficacy of MEK and RTK inhibitor therapies in a mouse model of KRAS-driven pancreatic cancer. *Cancer Res, 75*(6), 1091-1101. https://doi.org/10.1158/0008-5472.Can-14-1854

Pfaffl, M. W. (2001, May 1). A new mathematical model for. *Nucleic Acids Res, 29*(9), e45. https://www.ncbi.nlm.nih.gov/pmc/articles/PMC55695/pdf/gne045.pdf

Prahallad, A., Sun, C., Huang, S., Di Nicolantonio, F., Salazar, R., Zecchin, D., Beijersbergen, R. L., Bardelli, A., & Bernards, R. (2012, Jan 26). Unresponsiveness of colon cancer to BRAF(V600E) inhibition through feedback activation of EGFR. *Nature, 483*(7387), 100-103. https://doi.org/10.1038/nature10868

Puck, T. T., & Marcus, P. I. (1956, May 1). Action of x-rays on mammalian cells. *J Exp Med, 103*(5), 653-666. http://jem.rupress.org/content/jem/103/5/653.full.pdf

Quante, A. S., Ming, C., Rottmann, M., Engel, J., Boeck, S., Heinemann, V., Westphalen, C. B., & Strauch, K. (2016, Sep). Projections of cancer incidence and cancer-related deaths in Germany by 2020 and 2030. *Cancer Med, 5*(9), 2649-2656. https://doi.org/10.1002/cam4.767

Rahib, L., Smith, B. D., Aizenberg, R., Rosenzweig, A. B., Fleshman, J. M., & Matrisian, L. M. (2014, Jun 1). Projecting cancer incidence and deaths to 2030: the unexpected burden of thyroid, liver, and pancreas cancers in the United States. *Cancer Res, 74*(11), 2913-2921. https://doi.org/10.1158/0008-5472.CAN-14-0155

Rahib, L., Wehner, M. R., Matrisian, L. M., & Nead, K. T. (2021, Apr 1). Estimated Projection of US Cancer Incidence and Death to 2040. *JAMA Netw Open, 4*(4), e214708. https://doi.org/10.1001/jamanetworkopen.2021.4708

Raina, K., Lu, J., Qian, Y., Altieri, M., Gordon, D., Rossi, A. M., Wang, J., Chen, X., Dong, H., Siu, K., Winkler, J. D., Crew, A. P., Crews, C. M., & Coleman, K. G. (2016, Jun 28). PROTAC-induced BET protein degradation as a

therapy for castration-resistant prostate cancer. *Proc Natl Acad Sci U S A, 113*(26), 7124-7129. https://doi.org/10.1073/pnas.1521738113

Rajurkar, M., Dang, K., Fernandez-Barrena, M. G., Liu, X., Fernandez-Zapico, M. E., Lewis, B. C., & Mao, J. (2017, Jan 15). IKBKE Is Required during KRAS-Induced Pancreatic Tumorigenesis. *Cancer Res, 77*(2), 320-329. https://doi.org/10.1158/0008-5472.Can-15-1684

Rambow, F., Rogiers, A., Marin-Bejar, O., Aibar, S., Femel, J., Dewaele, M., Karras, P., Brown, D., Chang, Y. H., Debiec-Rychter, M., Adriaens, C., Radaelli, E., Wolter, P., Bechter, O., Dummer, R., Levesque, M., Piris, A., Frederick, D. T., Boland, G., Flaherty, K. T., van den Oord, J., Voet, T., Aerts, S., Lund, A. W., & Marine, J. C. (2018, Aug 9). Toward Minimal Residual Disease-Directed Therapy in Melanoma. *Cell, 174*(4), 843-855.e819. https://doi.org/10.1016/j.cell.2018.06.025

Rathert, P., Roth, M., Neumann, T., Muerdter, F., Roe, J. S., Muhar, M., Deswal, S., Cerny-Reiterer, S., Peter, B., Jude, J., Hoffmann, T., Boryn, L. M., Axelsson, E., Schweifer, N., Tontsch-Grunt, U., Dow, L. E., Gianni, D., Pearson, M., Valent, P., Stark, A., Kraut, N., Vakoc, C. R., & Zuber, J. (2015, Sep 24). Transcriptional plasticity promotes primary and acquired resistance to BET inhibition. *Nature, 525*(7570), 543-547. https://doi.org/10.1038/nature14898

Sarbassov, D. D., Guertin, D. A., Ali, S. M., & Sabatini, D. M. (2005). Phosphorylation and Regulation of Akt/PKB by the Rictor-mTOR Complex. *Science, 307*(5712), 1098-1101. https://doi.org/10.1126/science.1106148

Saxton, R. A., & Sabatini, D. M. (2017, Mar 9). mTOR Signaling in Growth, Metabolism, and Disease. *Cell, 168*(6), 960-976. https://doi.org/10.1016/j.cell.2017.02.004

Sen, T., Tong, P., Diao, L., Li, L., Fan, Y., Hoff, J., Heymach, J. V., Wang, J., & Byers, L. A. (2017, Oct 15). Targeting AXL and mTOR Pathway Overcomes Primary and Acquired Resistance to WEE1 Inhibition in Small-Cell Lung Cancer. *Clin Cancer Res, 23*(20), 6239-6253. https://doi.org/10.1158/1078-0432.Ccr-17-1284

Shimamura, T., Chen, Z., Soucheray, M., Carretero, J., Kikuchi, E., Tchaicha, J. H., Gao, Y., Cheng, K. A., Cohoon, T. J., Qi, J., Akbay, E., Kimmelman, A. C., Kung, A. L., Bradner, J. E., & Wong, K. K. (2013, Nov 15). Efficacy of BET bromodomain inhibition in Kras-mutant non-small cell lung cancer. *Clin Cancer Res, 19*(22), 6183-6192. https://doi.org/10.1158/1078-0432.Ccr-12-3904

Shu, S., Lin, C. Y., He, H. H., Witwicki, R. M., Tabassum, D. P., Roberts, J. M., Janiszewska, M., Huh, S. J., Liang, Y., Ryan, J., Doherty, E., Mohammed, H., Guo, H., Stover, D. G., Ekram, M. B., Brown, J., D'Santos, C., Krop, I. E., Dillon, D., McKeown, M., Ott, C., Qi, J., Ni, M., Rao, P. K., Duarte, M., Wu, S. Y., Chiang, C. M., Anders, L., Young, R. A., Winer, E., Letai, A., Barry, W. T., Carroll, J. S., Long, H., Brown, M., Liu, X. S., Meyer, C. A., Bradner, J. E., & Polyak, K. (2016, Jan 21). Response and resistance to BET bromodomain inhibitors in triple-negative breast cancer. *Nature, 529*(7586), 413-417. https://doi.org/10.1038/nature16508

Siegel, R. L., Miller, K. D., Fuchs, H. E., & Jemal, A. (2021, Jan). Cancer Statistics, 2021. *CA Cancer J Clin, 71*(1), 7-33. https://doi.org/10.3322/caac.21654

Song, M. S., Salmena, L., & Pandolfi, P. P. (2012, Apr 4). The functions and regulation of the PTEN tumour suppressor. *Nat Rev Mol Cell Biol, 13*(5), 283-296. https://doi.org/10.1038/nrm3330

Stathis, A., & Bertoni, F. (2018, Jan). BET Proteins as Targets for Anticancer Treatment. *Cancer Discov, 8*(1), 24-36. https://doi.org/10.1158/2159-8290.Cd-17-0605

Stratikopoulos, E. E., Dendy, M., Szabolcs, M., Khaykin, A. J., Lefebvre, C., Zhou, M. M., & Parsons, R. (2015, Jun 8). Kinase and BET Inhibitors Together Clamp Inhibition of PI3K Signaling and Overcome Resistance to Therapy. *Cancer Cell, 27*(6), 837-851. https://doi.org/10.1016/j.ccell.2015.05.006

Stratikopoulos, E. E., & Parsons, R. E. (2016, Jun 1). Molecular Pathways: Targeting the PI3K Pathway in Cancer-BET Inhibitors to the Rescue. *Clin Cancer Res, 22*(11), 2605-2610. https://doi.org/10.1158/1078-0432.Ccr-15-2389

Su, J. L., Yen, C. J., Chen, P. S., Chuang, S. E., Hong, C. C., Kuo, I. H., Chen, H. Y., Hung, M. C., & Kuo, M. L. (2007, 2007/02/01). The role of the VEGF-C/VEGFR-3 axis in cancer progression. *British Journal of Cancer, 96*(4), 541-545. https://doi.org/10.1038/sj.bjc.6603487

Subramanian, A., Tamayo, P., Mootha, V. K., Mukherjee, S., Ebert, B. L., Gillette, M. A., Paulovich, A., Pomeroy, S. L., Golub, T. R., Lander, E. S., & Mesirov, J. P. (2005, Oct 25). Gene set enrichment analysis: a knowledge-based approach for interpreting genome-wide expression profiles. *Proc Natl Acad Sci U S A, 102*(43), 15545-15550. https://doi.org/10.1073/pnas.0506580102

Sun, B., Fiskus, W., Qian, Y., Rajapakshe, K., Raina, K., Coleman, K. G., Crew, A. P., Shen, A., Saenz, D. T., Mill, C. P., Nowak, A. J., Jain, N., Zhang, L., Wang, M., Khoury, J. D., Coarfa, C., Crews, C. M., & Bhalla, K. N. (2018, 2018/02/01). BET protein proteolysis targeting chimera (PROTAC) exerts potent lethal activity against mantle cell lymphoma cells. *Leukemia, 32*(2), 343-352. https://doi.org/10.1038/leu.2017.207

Tamkun, J. W., Deuring, R., Scott, M. P., Kissinger, M., Pattatucci, A. M., Kaufman, T. C., & Kennison, J. A. (1992, Feb 7). brahma: a regulator of Drosophila homeotic genes structurally related to the yeast transcriptional activator SNF2/SWI2. *Cell, 68*(3), 561-572. https://www.cell.com/cell/pdf/0092-8674(92)90191-E.pdf?_returnURL=https%3A%2F%2Flinkinghub.elsevier.com%2Fretrieve%2Fpii%2F009286749290191E%3Fshowall%3Dtrue

Tiago, M., Capparelli, C., Erkes, D. A., Purwin, T. J., Heilman, S. A., Berger, A. C., Davies, M. A., & Aplin, A. E. (2020, Mar). Targeting BRD/BET proteins inhibits adaptive kinome upregulation and enhances the effects of BRAF/MEK inhibitors in melanoma. *Br J Cancer, 122*(6), 789-800. https://doi.org/10.1038/s41416-019-0724-y

Ueno, Y., Mori, M., Kamiyama, Y., Saito, R., Kaneko, N., Isshiki, E., Kuromitsu, S., & Takeuchi, M. (2019, Apr 2). Evaluation of gilteritinib in combination with chemotherapy in preclinical models of FLT3-ITD(+) acute myeloid

leukemia. *Oncotarget, 10*(26), 2530-2545. https://doi.org/10.18632/oncotarget.26811

Vazquez, R., Licandro, S. A., Astorgues-Xerri, L., Lettera, E., Panini, N., Romano, M., Erba, E., Ubezio, P., Bello, E., Libener, R., Orecchia, S., Grosso, F., Riveiro, M. E., Cvitkovic, E., Bekradda, M., D'Incalci, M., & Frapolli, R. (2017, Jan 1). Promising in vivo efficacy of the BET bromodomain inhibitor OTX015/MK-8628 in malignant pleural mesothelioma xenografts. *Int J Cancer, 140*(1), 197-207. https://doi.org/10.1002/ijc.30412

Vincent, A., Herman, J., Schulick, R., Hruban, R. H., & Goggins, M. (2011, Aug 13). Pancreatic cancer. *Lancet, 378*(9791), 607-620. https://doi.org/10.1016/s0140-6736(10)62307-0

Wei, W., Shin, Y. S., Xue, M., Matsutani, T., Masui, K., Yang, H., Ikegami, S., Gu, Y., Herrmann, K., Johnson, D., Ding, X., Hwang, K., Kim, J., Zhou, J., Su, Y., Li, X., Bonetti, B., Chopra, R., James, C. D., Cavenee, W. K., Cloughesy, T. F., Mischel, P. S., Heath, J. R., & Gini, B. (2016, Apr 11). Single-Cell Phosphoproteomics Resolves Adaptive Signaling Dynamics and Informs Targeted Combination Therapy in Glioblastoma. *Cancer Cell, 29*(4), 563-573. https://doi.org/10.1016/j.ccell.2016.03.012

Whiteman, D. C., Webb, P. M., Green, A. C., Neale, R. E., Fritschi, L., Bain, C. J., Parkin, D. M., Wilson, L. F., Olsen, C. M., Nagle, C. M., Pandeya, N., Jordan, S. J., Antonsson, A., Kendall, B. J., Hughes, M. C. B., Ibiebele, T. I., Miura, K., Peters, S., & Carey, R. N. (2015, Oct). Cancers in Australia in 2010 attributable to modifiable factors: introduction and overview. *Aust N Z J Public Health, 39*(5), 403-407. https://doi.org/10.1111/1753-6405.12468

Wirth, M., Mahboobi, S., Kramer, O. H., & Schneider, G. (2016, Aug). Concepts to Target MYC in Pancreatic Cancer. *Mol Cancer Ther, 15*(8), 1792-1798. https://doi.org/10.1158/1535-7163.Mct-16-0050

Yadav, B., Wennerberg, K., Aittokallio, T., & Tang, J. (2015). Searching for Drug Synergy in Complex Dose-Response Landscapes Using an Interaction Potency Model. *Comput Struct Biotechnol J, 13*, 504-513. https://doi.org/10.1016/j.csbj.2015.09.001

Ye, J., Coulouris, G., Zaretskaya, I., Cutcutache, I., Rozen, S., & Madden, T. L. (2012). Primer-BLAST: A tool to design target-specific primers for polymerase chain reaction. *BMC Bioinformatics, 13*, 134. https://doi.org/10.1186/1471-2105-13-134

Zhang, Z., Lin, G., Yan, Y., Li, X., Hu, Y., Wang, J., Yin, B., Wu, Y., Li, Z., & Yang, X. P. (2018, Jun). Transmembrane TNF-alpha promotes chemoresistance in breast cancer cells. *Oncogene, 37*(25), 3456-3470. https://doi.org/10.1038/s41388-018-0221-4

Zuber, J., Shi, J., Wang, E., Rappaport, A. R., Herrmann, H., Sison, E. A., Magoon, D., Qi, J., Blatt, K., Wunderlich, M., Taylor, M. J., Johns, C., Chicas, A., Mulloy, J. C., Kogan, S. C., Brown, P., Valent, P., Bradner, J. E., Lowe, S. W., & Vakoc, C. R. (2011, Aug 3). RNAi screen identifies Brd4 as a therapeutic target in acute myeloid leukaemia. *Nature, 478*(7370), 524-528. https://doi.org/10.1038/nature10334

Supplementary information

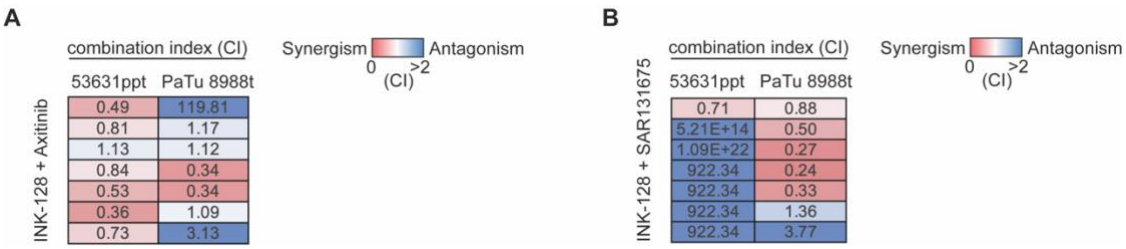

Supplemental Figure 1. Heatmap showing calculated CI values with one murine and one human cell line.

(A) Axitinib. (B) SAR131675.

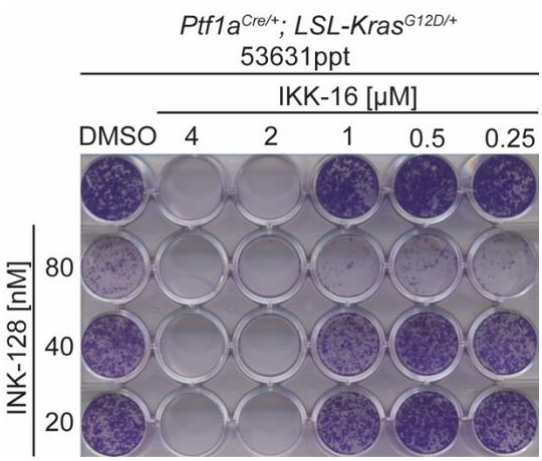

Supplemental Figure 2. Clonogenic assay replicate 2.

Clonogenic assay performed as a long-term viability assay with the indicated drug treatment.

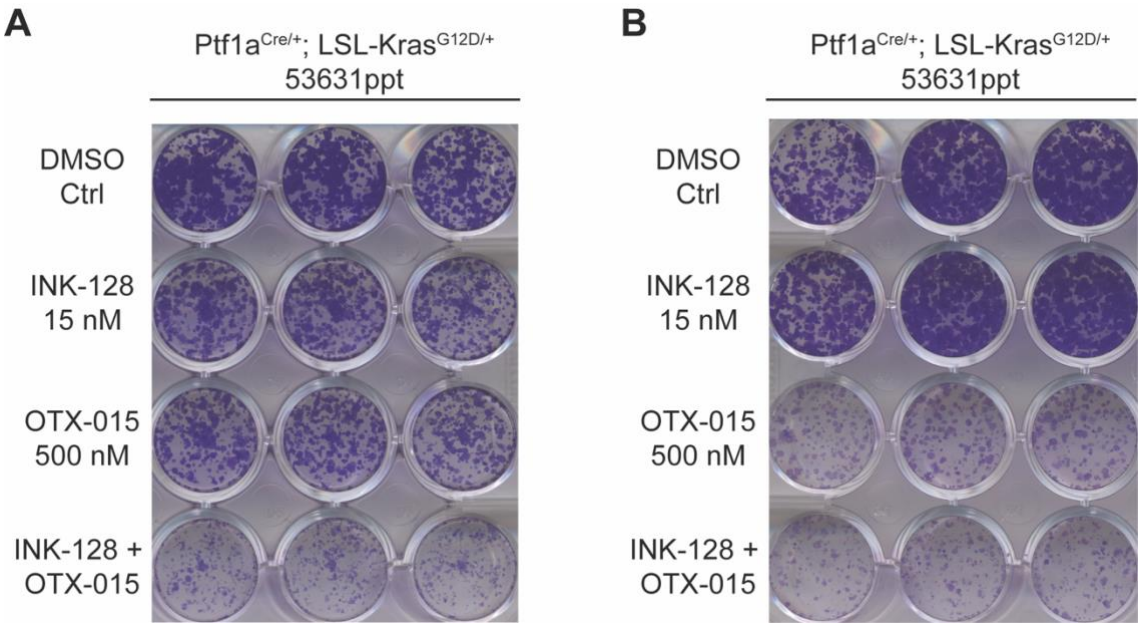

Supplemental Figure 3. MTOR-based combination therapy with OTX-015.

(A) – (B) Replicate 2 and 3 of the exemplary clonogenic assay treated with INK-128 15 nM and OTX-015 500 nM.

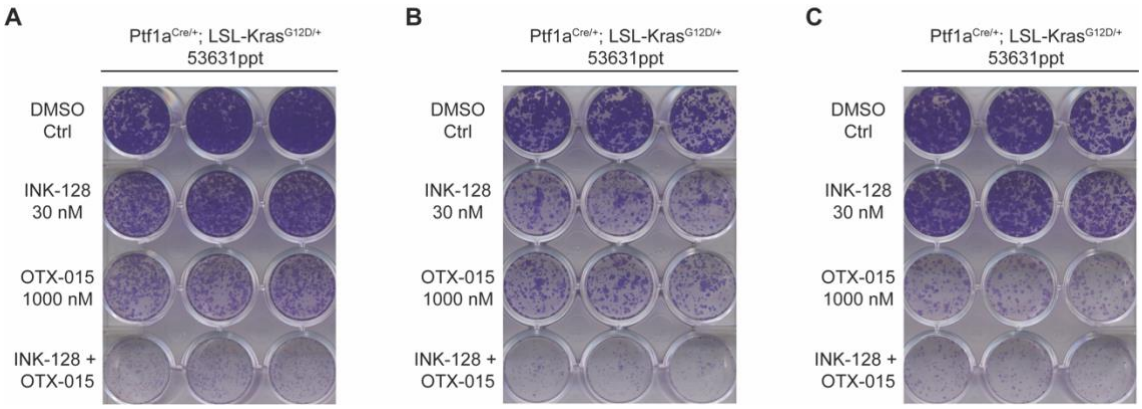

Supplemental Figure 4. Additional concentration of the MTOR-based combination therapy with OTX-015.

(A) – (C) 3 replicates of the clonogenic assay with twofold concentration (INK-128 30 nM, OTX-015 1000 nM) as showed in Figure 6E.

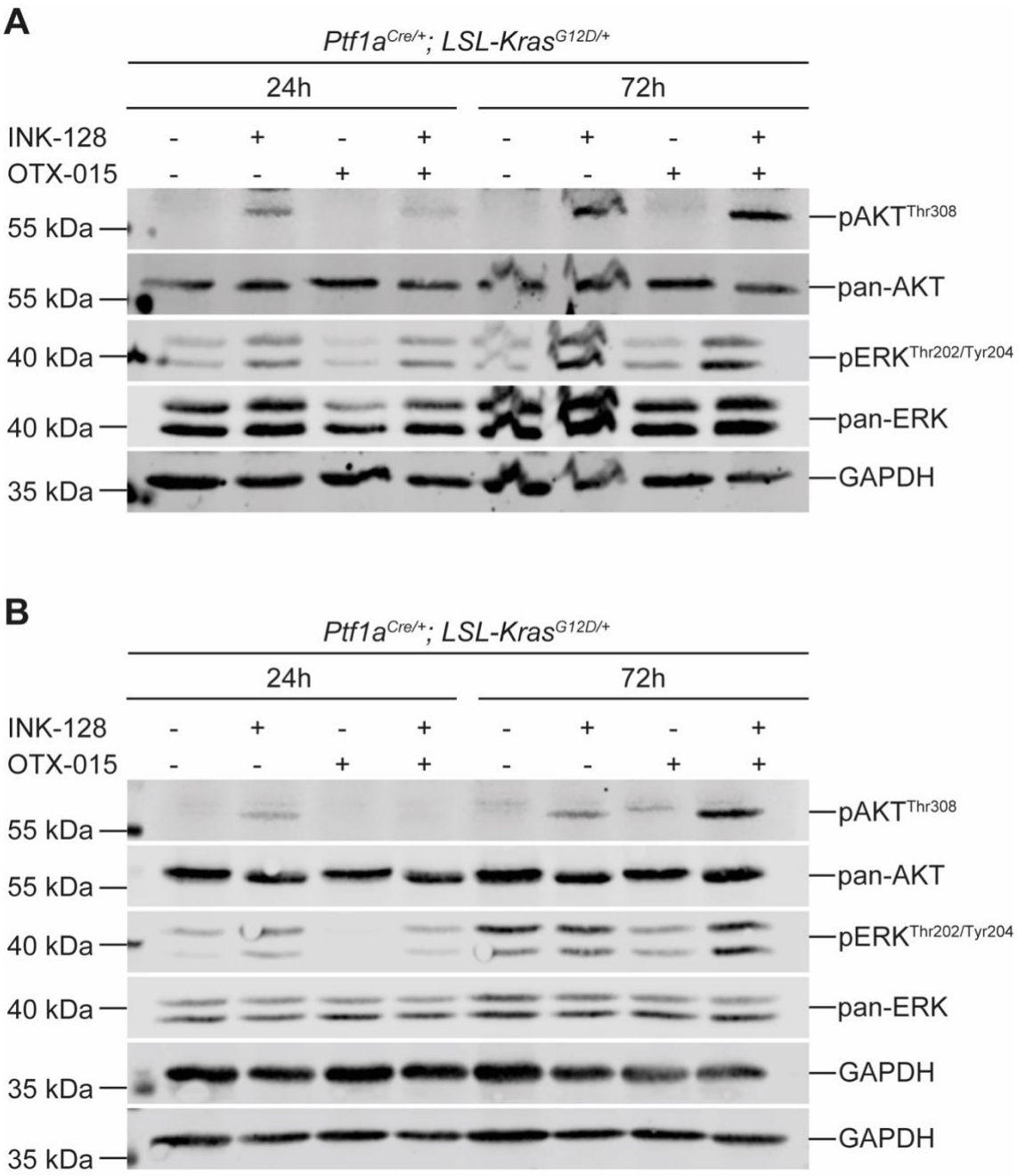

Supplemental Figure 5. Additional western blots for quantification.

(A) – (B) Ptf1a$^{Cre/+}$; LSL-Kras$^{G12D/+}$ cells were treated with INK-128 (500 nM), OTX-015 (1 µM) and the combination over indicated time. Western blot determines phosphorylation and expression of AKT (Thr308) as well as ERK (Thr202/Tyr204). Same lysates were blotted to different membranes and controlled by pan-AKT or pan-ERK for equal loading.

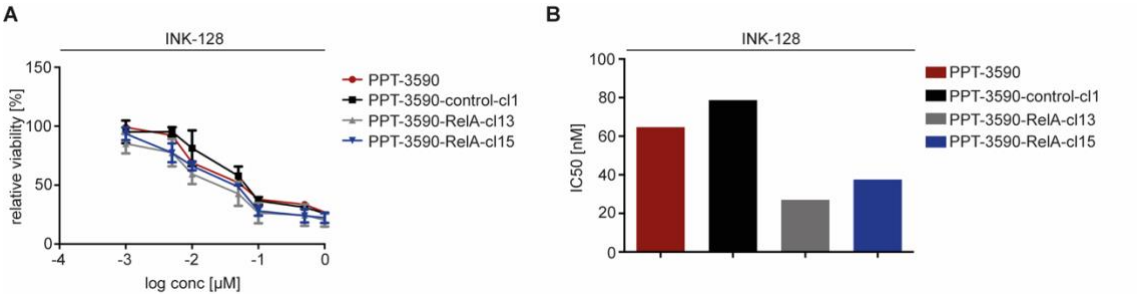

Supplemental Figure 6. Viability assay of RelA pro-/deficient clone upon MTORi.

(A) RelA proficient (PPT-3590-RelA-cl13, PPT-3590-RelA-cl15) and deficient (PPT-3590, PPT-3590-control-cl1) cell lines (Conradt et al., 2013) treated with INK-128 (1 - 1000 nM) for MTT assay. (B) Slight disparities of the cell line specific overall IC_{50} values.

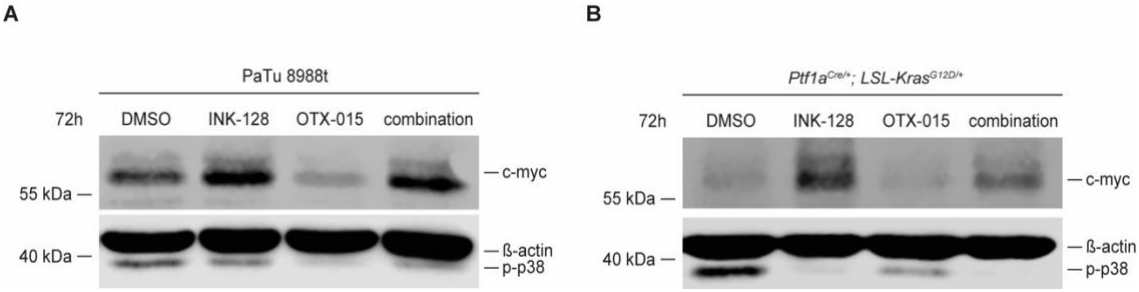

Supplemental Figure 7. Western blot illustrating c-myc upregulation upon MTOR inhibition.

(A) - (B) PaTu 8988t and Ptf1a$^{Cre/+}$; LSL-Kras$^{G12D/+}$ cells were treated with INK-128 (500 nM), OTX-015 (1 µM) and the combination over 72 hours. Western blot determines upregulation of c-myc after treatment with INK-128 and INK-128 + OTX-015 (n=1).